System Design and Outage Analysis for Cooperative Diversity Wireless Networks

by

Sungjoon Park

A dissertation submitted in partial fulfillment
of the requirements for the degree of
Doctor of Philosophy
(Electrical Engineering: Systems)
in The University of Michigan
2013

Doctoral Committee:

Professor Wayne E. Stark, Chair
Professor Kim A. Winick
Associate Professor Achilleas Anastasopoulos
Assistant Professor Branko Kerkez

ACKNOWLEDGEMENTS

Thanks to the people who made this dissertation possible, especially my advisor Wayne Stark for the useful comments, remarks and engagement through the learning process of this thesis. I would like to thank Prof. Winick, who conveyed an excitement in regard to teaching. Furthermore, I would like to express the deepest appreciation to my other committee members Prof. Anastasopoulos and Prof. Kerkez. Without their guidance and persistent help this dissertation would not have been possible.

I would also like to thank the financial support from the National Science Foundation Grant No. CCF-0910765, and the KAUST Global Collaborative Research Academic Excellence Alliance and Academic Partnership Programs.

It has been an exciting experience to study at the University of Michigan. I learned a lot from the great people I met in the state, from academic knowledge to wisdom of life. I would like to thank my loved ones in Korea as well, who have supported me throughout entire process, both by keeping me harmonious and helping me put the pieces together.

Lastly, I would like to express my utmost gratitude to my parents and my brother for their love and support, which have been a source of great comfort and energy throughout my graduate studies.

TABLE OF CONTENTS

LIST OF FIGURES

Figure

LIST OF ABBREVIATIONS

ACK acknowledgement

BRS best relay selection

CDMA code division multiple access

CSI channel state information

CSMA/CA carrier sense multiple access with collision avoidance

CTS clear-to-send

DIFS distributed interframe space

DSTC distributed space-time coding

DTRS dual-timer relay selection

FSRM full spatial reuse multi-hop

GPS global positioning system

HRS hybrid relay selection

MAC medium access control

MIMO multi-input-multi-output

MMRS max-max relay selection

MMSE minimum mean square error

OFDM orthogonal frequency division multiplexing

RRS receiver relay selection

RTS request-to-send

SIFS short interframe space

SINR signal-to-interference-and-noise ratio

SNR signal-to-noise ratio

TRS transmitter relay selection

ABSTRACT

System Design and Outage Analysis for Cooperative Diversity Wireless Networks

by

Sungjoon Park

Chair: Wayne E. Stark

Relay communication systems have recently been gaining momentum as an alternative to cellular architectures because of the ability to provide cost-efficient high spectral efficiency communications. The goal of this thesis is to investigate opportunistic relay communication strategies in various network configurations. We derive the outage probability of opportunistic multi-hop multiple relay networks with nodes having single or multiple antennas. The challenge in the analysis of the outage probability are in incorporating realistic channel effects such as path loss, shadowing, and fast fading. With these effects, the outage probability depends on the energy transmitted, and also the shadow fading characteristics. We incorporate the channel dynamics in analyzing opportunistic relay selection schemes and determine the optimal selection period.

As an extension of a conventional relay network, we explore a buffer-equipped relay network, where the network allows relays to delay transmission and transmit when the channel conditions are favorable. As a relay selection method, we suggest dual-timer relay selection (DTRS), which adopts the timer algorithm in reception and transmission relay selections. This algorithm reduces channel estimation overhead

and solves the full-buffer problem of a reception relay and the empty-buffer problem of a transmission relay in buffer-equipped networks. We further consider a spatial reuse multi-hop relay network, and propose a full spatial reuse multi-hop (FSRM) relay communication scheme, which allows relays to transmit their data using every other time slot. With the FSRM scheme, the end-to-end rate reduction factor of a multi-hop relay communication is fixed at 1/2, regardless of the number of hops. We provide a comprehensive analysis of the outage probability of the proposed scheme for a directional antenna system and an omnidirectional antenna system.

CHAPTER I

Introduction and Goals

1.1 Introduction

1.1.1 Cooperative Wireless Communication

Wireless communication is limited by the propagation characteristics of the environment. Generally, there are three effects that capture the propagation characteristics including path loss, shadowing, and fast fading [43]. Path loss is the attenuation of the signal strength with distance. This is usually modeled as an inverse power law where the received power decreases as the power of the distance between the transmitter and receiver. The second effect is the shadowing due to obstacles in the environment. This is usually modeled as a variation of the received signal power that has a lognormal distribution. This is sometimes called slow fading since its effect varies slowly due to a mobile node moving in relation to various obstacles. The third effect is fast fading in which the signal amplitude varies because of constructive and destructive interference between signals received along various propagation paths.

Various wireless communication schemes have been developed to overcome and exploit the wireless channel effects. If multiple paths, either using different time, frequency or space are possible, the probability of packet loss due to fading is significantly reduced. For instance, multiple paths with different delays gives rise to frequency se-

lective fading, which can be exploited to increase the transmission reliability in a wideband system such as orthogonal frequency division multiplexing (OFDM) and code division multiple access (CDMA). In multi-input-multi-output (MIMO) communication systems, spatial diversity gain can be achieved by generating signals with the same information at multiple antennas. However, in spite of the evolution of the wireless cellular technologies, the increase in the system complexity and the power consumption of modern wireless communication devices become practical issues.

Because of the increasing demand for cost-efficient high-rate wireless services, cooperative communication, which allows sharing use of common communication channels by multiple users, has been widely investigated. Cooperative communication is possible when there is at least one additional node willing to help in communication. In cooperative communication, such as relay communication, the signals are transmitted from multiple relays, which renders spatial diversity as in MIMO systems. In addition to the diversity gain, another advantage of relaying is that the total amount of radiated power necessary to communicate can be significantly reduced. The amount of power necessary to communicate a distance d is generally proportional to d^{η} where the path loss exponent η is typically 3 or 4. If a relay between the source and destination is available, then the distance between the source and the relay could be half the distance, which could require 1/16th of the power when η is 4. Of course the relay to the destination requires a similar amount of power. So the total transmitted power might get reduced by a factor of 8 by relaying.

The focus of this thesis is to study cooperative strategies and to investigate the advantages of various extensions of cooperative system. More specifically, we describe the architecture of a various cooperative systems and analyze the outage probability which helps us to understand the end-to-end system throughput incorporating potentially additional overhead for upper layers. Furthermore, as extensions of conventional cooperative systems, we employ a buffering and spatial-reuse concept to

improve overall system throughput.

1.1.2 Opportuistic Relay Communication

In cooperative networks, the outage probability of a channel is influenced by the number of relay nodes available in the network and the relaying protocol used. One of the widely investigated cooperative schemes is the distributed antenna system, which refers to a virtual MIMO comprising multiple antennas at the relays. In virtual MIMO systems, cooperative beamforming is investigated by weighting the virtual transmit and receive antenna patterns to be focused into a specific angular direction [31] [29]. In this protocol, beamforming the signals requires exchanging channel state information (CSI) between each relay, which needs additional resources and this overhead can be overwhelming in networks with many relays. To avoid this expense and achieve a diversity gain without knowing the global CSI, distributed space-time coding (DSTC) has been applied [25] [42]. However, in the absence of the global CSI at each node, using a single relay that provides the best end-to-end path between source and destination, which is called opportunistic relaying, achives the higher capacity than DSTC [10]. In addition, the opportunistic relaying simplifies receiver design and allows implementation with low-cost RF front-ends. In this regard, contrary to the multiple transmissions from several relay nodes, opportunistic relaying have been widely investigated for practical implementation [44] [8]. Research done to address issues in opportunistic relaying such as identifying the performance limits and selecting the best relay is described in [10] [40] and references therein. However, the channel model assumed in those papers only takes into account fast fading effects, and the selection method provided is not optimized to minimize the selection time.

Since the opportunistic relay communication strategies use a single relay, one could assume that an opportunistic relay selection requires CSI estimation of all relay links, and exchanging its information to a central controller or all involved

cooperating nodes. However, discovering the maximum channel gain relay among the set of multiple relays does not require the information of individual channel gain. Instead, a comparison logic is sufficient to discover the maximum or the minimum of the set. This observation naturally raises a problem of how to choose a maximum channel gain relay without exchanging exact CSI information.

There have been various approaches to select the optimal relay with local channel knowledge. One of the well received relay selection scheme is the splitting-based selection scheme [35][22]. In it, only the relays whose metrics lie between a threshold transmit in a slot. At the end of every time slot, a central controller broadcasts the outcome such as an idle, success, or collision to all the nodes. According to the outcome, the threshold is adjusted for the next time slot, and the algorithm continues until the outcome is a success. However, the algorithm complexity can be increased in a scale of the number of relays in the network. Another widely investigated algorithm is based on the distributed timer [9]. From the request-to-send (RTS) and clear-to-send (CTS) signals, each relay obtains their own channel gains. According to their channel gains, each relay sets a timer inversely proportional to their channel gains. The timer of the relay with the highest channel gain expires first, and that relay broadcasts a control signal that lets the other nodes know its timer has expired. Then the relay forwards the data to the destination. However, this algorithm also suffers from a collision in the relay selection phase when there are multiple relays with similarly high channel gains. The collision can be avoided by increasing differences between each relay's initial timer values. This is possible by increasing the initial timer scaling factor. However, as the scaling factor increases, the average relay selection time also increases, which potentially degrades the overall system throughput. Therefore, the initial timer scaling factor should be carefully chosen considering this tradeoff between the collision probability and the relay selection time. Research that has adopted the timer algorithm is presented in [10] and [19]. However, in [19] the

initial timer scaling factor is a constant set to be the length of distributed interframe space (DIFS).

Wireless communication not only occurs in short range scenarios, but also in wide area environment like a moving car in a rural environment. Thus, wireless services require a ubiquitous mobile radio system that considers mobility of mobile users. Since the mobility of users affects the channel dynamics, incorporating the channel dynamics, determining how often a relay selection algorithm should be executed becomes a crucial issue in a relay selection mechanism. For the channel model that we are assuming, the mobility affects the shadow fading time correlation. If the shadow fading is highly correlated across codewords, once the maximum channel gain relay is chosen, where it is optimal in terms of the outage probability, it is likely to be chosen again in the next transmission sequence. In this case, executing the selection algorithm at every packet transmission will be a waste of resources. Also, even if the selected relay is not optimal in the following transmission, if the channel gain difference between the optimal one and the previously selected one is small, using the previously selected one may still be optimal in the sense of throughput. This is because selecting a relay requires time resources and this could degrade the overall throughput. These observations indicate there is a throughput maximizing optimal time period in a relay selection to be performed. However, in most of literature on networks with multiple relays, consideration of the relay selection period is lacking. For instance, in [9], it is mentioned that their suggested distributed relay selection algorithm should be executed as often as the channel changes. However, the channel they are considering is a simple block fading and the corresponding selection period considering the channel dynamics is not addressed. In [38], a splitting-based algorithm for relay selection is analyzed and the tradeoff between the relay selection and the selection energy consumption is found. However, the analysis focuses on the optimal time duration for relay selection, because the suggested algorithm could be more

accurate if more time is allowed in the selection. The issue of how often does the algorithm have to be executed is lacking as well.

In this thesis, we find the exact point-to-point outage probability of the opportunistic relay communication considering the aforementioned channel effects. We will also find a high signal-to-noise ratio (SNR) approximation to the outage probability. We extend the findings of the single antenna relay network into a multi-antenna relay network incorporating the aforementioned mixed channel effects. Based on the understanding of point-to-point communication fundamental limits, we investigate the limits of a relay communication system. It has been proved in [10] that the proactive (relay selection before the source transmission) and the reactive (relay selection after the source transmission) relay selection have the same outage probability on a Rayleigh block fading channel. We show this result is valid also for the channel model with the mixed fading effects. We further analyze the collision probability of the distributed timer algorithm suggested in [9], and propose a collision resolving protocol. Considering the collision probability and the collision resolving protocol, we find the optimal timer scaling factor and the corresponding average relay selection time. We also find the optimal relay selection period that maximizes the end-to-end system throughput considering the average relay selection time and the shadow fading correlation property.

1.1.3 Buffer-equipped Relay Communication

Conventional relaying protocols employ a fixed schedule for reception and transmission. Thus, the relay selection scheme chooses a relay that maximizes the minimum of the channel gains between the source to relay and relay to the destination link where this selection method is called best relay selection (BRS) in [23]. However, there can be other relays with a higher source to relay or relay to destination channel gain than the relay that BRS selects. For the delay-unconstrained case, adaptive link

selection is possible using buffers where data can be queued until the relay to destination link is selected for transmission. As a link selection protocol, max-max relay selection (MMRS) has been suggested in buffer-equipped relay networks [23]. In the MMRS adopted network, the selected relay for the reception receives the source data and stores the data in a buffer. The selected relay for the transmission forwards the data in its buffer to the destination. For MMRS to work, the reception relay's buffer must not be filled and the transmission relay's buffer must not be empty. To resolve this restriction, hybrid relay selection (HRS) has been suggested in [23], so that when the aforementioned two cases occur, MMRS is adopted; otherwise, BRS is adopted. However, between the relay with the maximum source to relay channel gain and the relay that BRS selects, there can be other relays without the buffer issue. The same holds true for the relay to destination link. The performance of using one of those relays is lower bounded by using BRS because the buffer of the relay that BRS selects is never full or empty. Furthermore, in [23], relay selection is made by incorporating all the links' CSI, which involves feedback overhead from relays.

In this thesis, we address the issues of centralized relay selection and the full or empty buffer problem in MMRS by using the timer-based relay selection algorithm [10]. To the best of our knowledge, this algorithm has never been incorporated in the MMRS protocol. We call the timer-based MMRS a DTRS algorithm since it requires two timers at each node. In the DTRS algorithm, the receiver relay selection (RRS) is executed using the source to relay channel gain, and the transmitter relay selection (TRS) is performed by using the relay to destination channel gain. Each selection is based on the distributed timer algorithm, but the difference is that relays with a full buffer do not set their timer in the RRS phase and relays with an empty buffer are excluded in the TRS phase. Therefore, the DTRS algorithm resolves buffer issues in the MMRS protocol and does not require the overhead of CSI feedback from relays.

1.1.4 Spatial Reuse Multi-hop Relay Communication

In conventional multi-hop networks, each node in the network accesses the channel in a different time slot. However, because wireless channel resources are limited, multi-hop relay networks that allow for spatial reuse have been investigated [2][20]. In spatial reuse multi-hop relay networks, the system capacity is improved by scheduling of multiple nodes to transmit in a same time slot. Research conducted to address issues in spatial reuse multi-hop relay communication strategy is described in [5] [45] and references therein. For instance, in [5], the end-to-end energy consumption and bandwidth efficiency are analyzed, and the optimal energy-bandwidth tradeoff with a spatial reuse strategy is examined. The spatial reuse strategy suggested in [5] allows concurrent transmissions to relays separated by at least 3 hops, which does not maximize channel utilization. In addition, the end-to-end bandwidth efficiency analysis is restricted to an AWGN channel. In [45], the authors find the optimal spatial reuse factor that maximizes the network throughput. However, according to their findings, when the spatial reuse factor is 2 (allowing concurrent transmissions to relays separated by 2 hops), the network throughput is close to zero because of the high interference level. Research on more aggressive spatial reuse strategies with a realistic channel model has not yet been undertaken.

As an aggressive spatial reuse strategies, we suggest a FSRM relaying scheme which allows simultaneous transmissions to relays separated by 2 hops. However, simultaneous transmission by nearby nodes gives rise to co-channel interference, which is a key factor in system performance degradation. To overcome this limitation, we investigate an interference management scheme with a power allocation strategy.

1.2 Outline of Thesis

In the following chapters, we present our proposal for a practical cooperative diversity scheme and analyze its performance. The model for the channel that we consider includes path loss, shadowing, and fast fading. For this channel model, in chapter II, we first aim to study the point-to-point outage probability of a single antenna network. As an extension of a single antenna network, we explore a multi-antenna network incorporating the mixed channel effects. Based on the point-to-point outage probability analysis, we derive an outage probability of opportunistic two-hop multiple relay network.

We study the optimization over a relay selection in chapter III. This relay selection can cause additional transmission of control signals in medium access control (MAC) layer. To minimize the outage probability and MAC layer overhead, we consider an opportunistic timer based relay selection algorithm suggested by A. Bletsas [10]. We find the optimal parameter for the algorithm that minimizes the relay selection time and suggest a collision resolving mechanism. Considering the channel dynamics, we further investigate the optimal relay selection period to maximize the throughput while avoiding selection overhead.

In chapter IV, we analyze a multi-hop relay network performance in terms of throughput maximizing optimal number of hops and optimal rate. We first find the outage probability for the multi-hop relay communication strategy that allows a packet to follow any path through the relays in the network. Based on the outage probability and the rate that is used in the network, we find the exact throughput of the system. From this understanding of the system throughput, we find the optimal operating rate and the optimal number of hops that maximize the throughput.

In chapter V, we explore benefits of a buffer-equipped multi-hop relay network and compare the system throughput with the conventional multi-hop relay network without buffers. We also present a spatial reuse multi-hop relay scheme in this chapter.

We provide a comprehensive analysis of the outage probability of the proposed scheme for a directional antenna system and an omnidirectional antenna system. For an omnidirectional antenna system, we find the SNR region of the proposed scheme that achieves better performance. We further analyze various power allocation methods to manage interference and determine the optimal operation scheme in terms of the signal-to-interference-and-noise ratio (SINR). Our conclusions with useful insights and open research issues are identified and discussed in chapter VI.

CHAPTER II

Opportunistic Relay Communication in Fast and Slow Fading Channels

2.1 Introduction

Communication of a single source to a single destination without the cooperation of any other communicating nodes is called direct or point-to-point communication. As in point-to-point communication systems, it is important to understand the fundamental limit of relay communication systems. That is, what is the maximum rate that reliable communications can take place between a source and destination pair when using a relay. The challenges in the analysis of the fundamental limit are in incorporating realistic channel effects such as propagation loss, shadowing, and fast fading. With these effects, the fundamental limit on the rate of communication is a function of the energy transmitted, but it is also a function of the particular shadowing between the source, relay and destination. Since the shadowing can change from one codeword to another, the probability that the rate of the code used exceeds the capacity is a useful measure of performance. This is called the outage probability. There have been attempts to find a simple formula for the outage probability of the channel with the aforementioned three effects [32][27]. For instance, in [27], the suggested outage formula assumes that fast and slow fading are both random but

constant over an entire codeword. However, it is more realistic to assume that the fast fading varies within a codeword because the coherence time or coherence bandwidth is much smaller than the packet length or signal bandwidth.

The use of multiple antennas in point-to-point communication is one of the most important techniques for increasing the data rate of existing wireless systems and also for emerging wireless systems such relay communication. We first need a good understanding of the MIMO propagation channel that also incorporates realistic channel effects. In a MIMO channel, the performance depends on knowledge at the transmitter or receiver about the state of the channel. Further, whether the information is the instantaneous channel gain or a statistical knowledge of the channel, the analytical framework can be different. The fundamental limits of a MIMO channel were addressed in [21] [13] and references therein. However, the channel model assumed only captures fast fading effects, and the analysis is restricted to the maximum transmission rate. For the channel model that we assume in this thesis, the fundamental limit is a function of shadow fading level, as in single antenna networks. Thus, an outage probability is a meaningful performance measure.

In recent years, interest in relay networks with multiple-antenna nodes has increased, because of the significant enhancement of spectral efficiency and link reliability compared to MIMO networks without relays and to relay networks without multiple-antenna nodes [7] [46]. There have been efforts to find a capacity achieving MIMO relay communication protocol with low complexity. In [11], for example, a maximum capacity achieving protocol was proposed in which relays fully cooperate to orthogonalize the MIMO channel by joint decoding and interstream interference cancellation at the relay nodes. In this protocol, however, this relay cooperation requires that all the nodes know the global CSI, necessitating additional resources to forward CSI. To avoid this expense, a near-optimal low-complexity antenna selection scheme has been investigated [46]. This cooperation protocol finds the optimal anten-

nas set distributed on multiple relays, where the selection is made opportunistically by sorting the singular values of every relay's channel gain matrix. However, in the channel and system model that we are assuming, where the nodes have the same number of antennas, using the best relay minimizes the outage probability of the network since the outage probability depends solely on the shadow fading level and the statistics of the fast fading (a detailed proof is provided in Section 2.3.2). Therefore, opportunistic relaying strategy needs to be investigated in MIMO relay networks.

In this chapter we focus on the outage probability of a point-to-point communication where the mixed channel effects are accounted. We show how the mixed channel effects are included in a MIMO implementation. We analyze the outage probability of an opportunistic relay network and present a numerical analysis for various network configurations.

2.2 Single Antenna Point-to-Point Communication

2.2.1 Channel Model

The channel model considered takes into account path loss, shadowing and fast fading effects. We assume the transmitter nodes have knowledge of channel statistics but not the channel realization information. Suppose that the number of coherence periods in a codeword is K as shown in Fig. 2.1, then the transmitted signal and received signal are related as

$$y[k] = \frac{h[k]\sqrt{L}}{d^{\frac{\eta}{2}}}\sqrt{\mathrm{E}}x[k] + w[k], \qquad k = 1, ..., K \tag{2.1}$$

where $k = 1, ..., K$ represents an index of the coherence period, $x[k]$ and $y[k]$ are k-th transmitted and received symbols, respectively. There can be multiple symbols per coherence period, but we are assuming that coding is done over K such coherence periods, thus consecutive symbols will experience different coherence periods. The

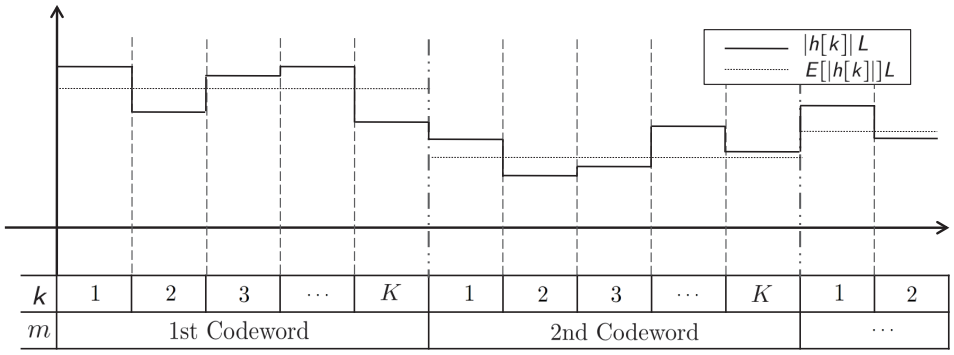

Figure 2.1: Example of channel dynamics

constant d is the distance between the transmitter and receiver, η is the path loss exponent, and E is the average energy per transmitted symbol. The noise component $w[k]$ is i.i.d. $\mathcal{CN}(0, N_0)$. The fast fading component, $|h[k]|^2$, is a Rayleigh distributed random variable (r.v.) with $E[|h[k]|^2] = 1$. Also, $|h[k]|^2$ is constant over the k-th coherence period and i.i.d. across different coherence periods. The r.v. L represents the slow fading component and is modeled as a lognormal r.v., where $\ln(L)$, we denote Γ, is $\mathcal{N}(0, \sigma^2)$. The corresponding mean and the variance of L is defined as follows

$$E[L] = e^{\sigma^2/2}, \qquad \text{Var}[L] = e^{2\sigma^2} - e^{\sigma^2}.$$

We will denote the shadow fading level of m-th codeword from node i to j by $L_{m,ij}$, and drop subscripts when there is no confusion. The slow fading component can be modeled as a first order autoregressive discrete time random process, where we assume that the shadow fading level L remains constant over a codeword, but is correlated from one codeword to another codeword. The correlation coefficient of $\Gamma_1 = \ln(L_1)$ and $\Gamma_m = \ln(L_m)$, is modeled as [17],

$$\rho((m-1)\tau) = E\left[\frac{\Gamma_1 \Gamma_m}{\sigma^2}\right] = {\epsilon_d}^{(m-1)\tau v/d}, \tag{2.2}$$

where σ is the standard deviation of Γ_1 and Γ_m, τ is the duration of a codeword transmission, v is the velocity of a mobile node, and ϵ_d is the correlation between two points separated by distance d. Since ϵ_d is less than 1, we observe that the correlation decreases as the velocity increases.

In Fig. 2.1 the solid line represents an example of the combination of fast and slow fading channel dynamics $|h[k]|^2 L$, and the dotted line represents slow fading channel dynamics L. According to this channel dynamics, the average received SNR, denoted by γ, is defined as

$$\gamma = E_{|h[k]|^2, L}\left[\frac{\mathrm{E}|h[k]|^2 L}{d^\eta N_0}\right] = \frac{\mathrm{E}E[L]}{d^\eta N_0}.$$

2.2.2 Outage Probability Analysis

In this section a closed form expression for the capacity and the outage probability of the channel model described in the previous section is derived. Suppose information is coded and the coded symbols are separated over a coherence period. We can view the channel as K parallel sub-channels that fade independently given the slow fading level. An outage occurs when the target rate R (in bits/s/Hz) per sub-channel is greater than the capacity of the channel. When the codeword is long, thus K is large, the law of large numbers can be invoked to approximate the outage probability of the channel as follows (dropping index k) [43]

$$P_{out}(R) = Pr\left(E_{|h|^2}\left\{\log\left(1 + |h|^2 L\gamma\right)\right\} < R\right). \tag{2.3}$$

The expectation in (2.3) is only taken with respect to the fast fading $|h|$. Here we assume the destination knows the fast fading and the slow fading realization, and the transmitter knows the statistical information of both fadings. We denote the

expectation term in (2.3) as $C(L)$. This expectation can be computed as

$$\begin{aligned} C(L) &= E_{|h|^2}\left\{\log\left(1+|h|^2 L\gamma\right)\right\} \\ &= \int_0^\infty \log\left(1+xL\gamma\right)e^{-x}dx \\ &= -\frac{e^{\frac{1}{L\gamma}}}{\ln 2} Ei\left(-\frac{1}{L\gamma}\right), \end{aligned} \tag{2.4}$$

where $Ei(x)$ is exponential integral defined by

$$Ei(x) = -\int_{-x}^{\infty} \frac{e^{-t}}{t} dt. \tag{2.5}$$

Using a Taylor series expansion for the exponential term e^{-t}/t, the exponential integral can be written as

$$Ei(x) = \alpha + \ln|x| + \sum_{l=1}^{\infty} \frac{x^l}{l \cdot l!}, \tag{2.6}$$

where α is the Euler-Mascheroni constant, which is approximately 0.58. In the high SNR regime, the argument of the exponential integral of (2.6) become small. Thus we can approximate the series by a finite number of terms. By substituting (2.6) into (2.4) and approximating the series by terms up to the second order, (2.4) becomes

$$\begin{aligned} C(L) &= E_{|h|^2}\left\{\log\left(1+|h|^2 L\gamma\right)\right\} \\ &\approx \frac{e^{\frac{1}{L\gamma}}}{\ln 2}\left(\ln(L\gamma) + \frac{1}{L\gamma} - \frac{1}{4(L\gamma)^2} - \alpha\right) = \widetilde{C}(L), \end{aligned} \tag{2.7}$$

where we denote the capacity approximation (2.7) as $\widetilde{C}(L)$. Then the corresponding outage probability (2.3) is approximately given by

$$P_{out}(R) \approx Pr(\widetilde{C}(L) < R).$$

Although finding the algebraic expression for the inverse function of $C(L)$ and $\widetilde{C}(L)$ is difficult, we can find them numerically since they are monotonic increasing functions. We denote the inverse functions as $g(R)$ and $\widetilde{g}(R)$ respectively. Then, the outage probability for a single link can be approximated as

$$\begin{aligned} P_{out}(R) &= Pr(C(L) < R) \\ &= Pr(L < g(R)) \\ &= 1 - Q\left(\frac{\ln(g(R))}{\sigma}\right) \\ &\approx 1 - Q\left(\frac{\ln(\widetilde{g}(R))}{\sigma}\right). \end{aligned}$$

The accuracy of the approximation is analyzed in Section 2.5, where we show it matches the exact outage probability in the high SNR region as well as in the low SNR region.

2.3 Multiple Antenna Point-to-Point Communication

2.3.1 Channel Model

For the channel model, we assume that the number of antennas at every node is the same, but we will use N_S,N_R and N_D to denote the number of antennas at the source, relays, and destination, respectively, n to denote $\max(N_S, N_D)$, and m to denote $\min(N_S, N_D)$ for analysis purposes. Given the channel effects, the received signal vector $\mathbf{y}$ at the destination node can be written as

$$\mathbf{y} = \frac{\sqrt{L}}{d^{\eta/2}}\mathbf{H}\mathbf{x} + \mathbf{w}, \tag{2.8}$$

where $\mathbf{x}$ is the transmitted symbol vector, and $\mathbf{w}$ is the noise which is i.i.d. $\mathcal{CN}(0, N_0\mathbf{I}_{N_D})$. The $N_D \times N_S$ matrix $\mathbf{H}$ is composed of h_{ij}, which is the fast fading channel gain from

transmitter antenna j to receiver antenna i. Each of h_{ij} is i.i.d. complex Gaussian r.v. with $E[|h_{ij}|^2] = 1$. The i.i.d. assumption is valid when the antenna is separated more than the coherence distance [41]. The random matrix $\mathbf{HH}^\dagger$ (if $N_D \leq N_S$ and $\mathbf{H}^\dagger\mathbf{H}$ if $N_D > N_S$) has full rank with probability 1 [43], and it has a complex central Wishart distribution. As in the single antenna channel model in (2.1), d is the distance between two nodes, η is the path loss exponent, and the shadow fading effect is captured by L with the same probabilistic character. We assume that the shadow fading affects all antennas equally since shadowing occurs in large spatial scales. This shadow fading component is modeled as a first order autoregressive discrete time random process, where the correlation coefficient is modeled as (2.2).

2.3.2 Outage Probability Analysis

In this section, we derive a closed form expression for the capacity and the outage probability of the point-to-point MIMO communication network. We assume that the CSI is available at the source and the destination. We also assume that there exists an average power constraint rather than a constraint for each channel realization. Power allocation, therefore, can be performed with respect to time and space. Since the contributions of shadowing effects at different antennas are the same, for the channel model that we are assuming, the achievable rate of MIMO communication is a function of the shadow fading level. We denote the achievable rate of the MIMO communication using the same notation $C(L)$ as a single antenna network as follows [16]

$$C(L) = \max_{E[\mathrm{tr}(\mathbf{Q})]\leq \mathrm{E}} E_{\mathbf{H}}\left[\log\det\left(I_{N_D} + \frac{L}{d^\eta N_o}\mathbf{HQH}^\dagger\right)\right], \tag{2.9}$$

where $\mathbf{Q} = E[\mathbf{xx}^\dagger]$, and E is the average power constraint. The outage probability is the probability that the achievable rate is smaller than the rate of the code used in

transmission [33], which is given as follows

$$P_{out}(R) = Pr(C(L) < R),$$

where R (in bits/s/Hz) is the rate of the code. To orthogonalize the channel vector, we apply singular value decomposition (SVD) of $\mathbf{H} = U\Lambda V^*$ to (2.8). Then the received signal $\mathbf{y}$ is alternatively described as follows

$$\tilde{\mathbf{y}} = \sqrt{\frac{L}{d^\eta}}\Lambda\tilde{\mathbf{x}} + \tilde{\mathbf{w}},$$

where $\tilde{\mathbf{y}} = U^*\mathbf{y}$, $\tilde{\mathbf{x}} = V^*\mathbf{x}$, $\tilde{\mathbf{w}} = U^*\mathbf{w}$ and $\Lambda = \text{diag}[\lambda_1, \lambda_2, ...\lambda_m]$, where λ_i is ith singular value of the matrix $\mathbf{H}$. Then the power allocation can be carried over $\tilde{\mathbf{Q}} = E[\tilde{\mathbf{x}}\tilde{\mathbf{x}}^\dagger]$ instead of $\mathbf{Q}$. The achievable rate (2.9) then becomes

$$\begin{aligned} C(L) &= \max_{E[\text{tr}(\tilde{\mathbf{Q}})]\leq \text{E}} \sum_{k=1}^{m} E\left[\log\left(1 + \frac{\lambda_k L\tilde{Q}_{kk}(\lambda_k)}{d^\eta N_o}\right)\right] \\ &= \max_{E[\text{tr}(\tilde{\mathbf{Q}})]\leq \text{E}} m\int_\lambda \log\left(1 + \frac{\lambda L\tilde{Q}(\lambda)}{d^\eta N_o}\right) f_\lambda(\lambda)d\lambda, \end{aligned} \tag{2.10}$$

where $\tilde{Q}_{kk}(\lambda_k)$ is the kth row and column element of matrix $\tilde{\mathbf{Q}}$, and $f_\lambda(\lambda)$ denotes the pdf of any unordered λ_k, which is derived in [41] as follows

$$f_\lambda(\lambda) = \frac{e^{-\lambda}\lambda^{n-m}}{m}\sum_{k=1}^{m}\frac{(k-1)!}{(n-m+k-1)!}\left[\Psi_{k-1}^{n-m}(\lambda)\right]^2. \tag{2.11}$$

In (2.11) $\Psi_k^a(\lambda)$ is the associated Laguerre polynomial of order k defined as

$$\begin{aligned} \Psi_k^a(\lambda) &= \frac{1}{k!}e^\lambda\lambda^{-a}\frac{d^k}{d\lambda^k}(e^{-\lambda}\lambda^{a+k}) \\ &= \sum_{i=0}^{k}(-1)^i\binom{k+a}{k-i}\frac{\lambda^i}{i!}. \end{aligned} \tag{2.12}$$

Using (2.12), the pdf of λ (2.11) can be expressed as follows

$$\begin{aligned} f_\lambda(\lambda) &= \frac{e^{-\lambda}\lambda^{n-m}}{m}\sum_{k=1}^{m}\frac{(k-1)!}{(n-m+k-1)!}\times\left[\Psi_{k-1}^{n-m}(\lambda)\right]^2 \\ &= \frac{e^{-\lambda}\lambda^{n-m}}{m}\sum_{k=1}^{m}\frac{(k-1)!}{(n-m+k-1)!} \\ &\times\left[\sum_{i=0}^{k-1}\sum_{j=0}^{k-1}(-1)^{i+j}\binom{n-m+k-1}{k-i}\binom{n-m+k-1}{k-j}\frac{\lambda^{i+j}}{i!j!}\right]. \end{aligned} \tag{2.13}$$

Given the power constraint $E[\mathrm{tr}(\mathbf{Q})] \leq \mathrm{E}$, the maximizing power allocation rule is shown to be the water-filling algorithm [16] which yields

$$\frac{\tilde{Q}(\lambda)}{\mathrm{E}/m} = \left[\frac{1}{\gamma_o}-\frac{1}{\gamma}\right]^+ \Rightarrow \frac{L\tilde{Q}(\lambda)}{d^\eta N_o} = \left[\frac{1}{\lambda_o}-\frac{1}{\lambda}\right]^+, \tag{2.14}$$

where x^+ denotes $\max\{0,x\}$, and λ_o and λ are the normalization of γ_o and γ by $L\mathrm{E}/d^\eta N_o m$. Applying (2.14) to (2.10) renders

$$C(L) = m\int_{\lambda_o}^{\infty}\log\left(\frac{\lambda}{\lambda_o}\right)f_\lambda(\lambda)d\lambda, \tag{2.15}$$

where the cutoff value λ_o is obtained by solving the integral equation

$$\int_{\lambda_o}^{\infty}\left(\frac{1}{\lambda_o}-\frac{1}{\lambda}\right)f_\lambda(\lambda)d\lambda = \frac{L\mathrm{E}}{d^\eta N_o m}. \tag{2.16}$$

The existence and the uniqueness of the solution above is shown in [24]. Using the pdf expression for λ in (2.13), the left hand side of (2.16) becomes

$$\int_{\lambda_o}^{\infty}\left(\frac{1}{\lambda_o}-\frac{1}{\lambda}\right)f_\lambda(\lambda)d\lambda$$

$$= \sum_{k=1}^{m} \frac{(k-1)!}{(n-m+k-1)!} \sum_{i=0}^{k-1} \sum_{j=0}^{k-1} \frac{(-1)^{i+j}}{i!j!} \binom{n-m+k-1}{k-i}$$
$$\times \binom{n-m+k-1}{k-j} \int_{\lambda_o}^{\infty} \left(\frac{1}{\lambda_o} - \frac{1}{\lambda} \right) e^{-\lambda} \lambda^{n-m+i+j} d\lambda. \tag{2.17}$$

The integration part in (2.17) is a well known gamma function form, where we define $\mathcal{L}(i, \lambda_o)$ as follows

$$\mathcal{L}(i, \lambda_o) = \int_{\lambda_o}^{\infty} e^{-\lambda} \lambda^{i-1} d\lambda = \sum_{l=0}^{i-1} \frac{(i-1)!}{l!} \lambda_o^l e^{-\lambda_o}.$$

When $n - m > 0$, using the gamma function, the integration part in (2.17) becomes as follows

$$\int_{\lambda_o}^{\infty} \left(\frac{1}{\lambda_o} - \frac{1}{\lambda} \right) e^{-\lambda} \lambda^{n-m+i+j} d\lambda$$
$$= \frac{\mathcal{L}(n-m+i+j+1, \lambda_o)}{\lambda_o} - \mathcal{L}(n-m+i+j, \lambda_o).$$

On the other hand, when $n = m$, the integration becomes as follows

$$\int_{\lambda_o}^{\infty} \left(\frac{1}{\lambda_o} - \frac{1}{\lambda} \right) e^{-\lambda} \lambda^{n-m+i+j} d\lambda = \frac{\mathcal{L}(1, \lambda_o)}{\lambda_o} - E_1(\lambda_o), \tag{2.18}$$

where $E_1(\lambda_o)$ is exponential integral defined by

$$E_1(\lambda_o) = \int_{1}^{\infty} \frac{e^{-\lambda_o t}}{t} dt.$$

In both cases, we can find λ_o numerically. Likewise, from (2.13), the capacity (2.15) becomes

$$C(L) = \sum_{k=1}^{m} \frac{(k-1)!}{(n-m+k-1)!} \sum_{i=0}^{k-1} \sum_{j=0}^{k-1} \frac{(-1)^{i+j}}{i!j!} \binom{n-m+k-1}{k-i} \times \binom{n-m+k-1}{k-j} \int_{\lambda_o}^{\infty} \log\left(\frac{\lambda}{\lambda_o}\right) e^{-\lambda} \lambda^{n-m+i+j} d\lambda, \tag{2.19}$$

where the integration is

$$\int_{\lambda_o}^{\infty} \log\left(\frac{\lambda}{\lambda_o}\right) e^{-\lambda} \lambda^{i} d\lambda = \log(e) \lambda_o^{n-m+i+j+1} \mathcal{J}_{n-m+i+j+1}(\lambda_o), \tag{2.20}$$

and

$$\mathcal{J}_n(\lambda_o) = \int_{1}^{\infty} t^{n-1} \ln t e^{-\lambda_o t} dt. \tag{2.21}$$

This equation is evaluated in [3] as follows

$$\mathcal{J}_n(\lambda_o) = \frac{(n-1)!}{\lambda_o^n} \left[E_1(\lambda_o) + \sum_{k=1}^{n-1} \frac{\mathcal{P}_k(\lambda_o)}{k} \right] \tag{2.22}$$

and

$$\mathcal{P}_k(\lambda_o) = e^{-\lambda_o} \sum_{q=0}^{k-1} \frac{\lambda_o^q}{q!}.$$

Although finding the capacity equation (2.19) is computationally intensive, and finding its algebraic expression for the inverse function is difficult, we can find this numerically since it is a monotonic increasing function. Since the capacity is a function of a shadow fading level as the single antenna analysis, we use the same notation $g(R)$ for the inverse function of $C(L)$ as in the single antenna analysis. Then, the outage

probability for a single link can be expressed as follows

$$\begin{aligned} P_{out}(R) &= Pr(C(L) < R) \\ &= 1 - Q\left(\frac{\ln(g(R))}{\sigma}\right). \end{aligned} \tag{2.23}$$

2.4 Relay Communication Performance Analysis

2.4.1 System Model

In this section, we consider a half-duplex two-hop relay communication system as shown in Fig. 2.2, comprised of a source node, N relay nodes $R_1, ..., R_N$ and a destination node sharing the same frequency band. Topology information regarding the location of each relay is obtained by some means of distance measurement either through specialized hardware such as global positioning system (GPS) or by measuring average signal strength. The protocol for transmitting information from the source to the destination uses two phases or time periods. As shown in Fig. 2.2, the source transmits the data in phase 1. The relays that successfully decode the received signal execute a relay selection algorithm. The optimal relay and the relay selection algorithm will be addressed in detail in the following sections. The chosen relay forwards the data packet to the destination in phase 2. If the relay is chosen before the source transmission, it is called a proactive relay selection. In this way, only the selected relay spends energy for reception, all the other relays that are not selected to forward the data can avoid listening to the source information. Thus, the proactive relay selection has an advantage of saving reception energy in the relay nodes which are not involved in forwarding the data. However, the opportunistic selection incorporates all the relays in the network, which increases complexity with the number of participating relays in the relay selection. On the other hand, as illustrated in Fig. 2.2, performing relay selection after the source transmission is called a

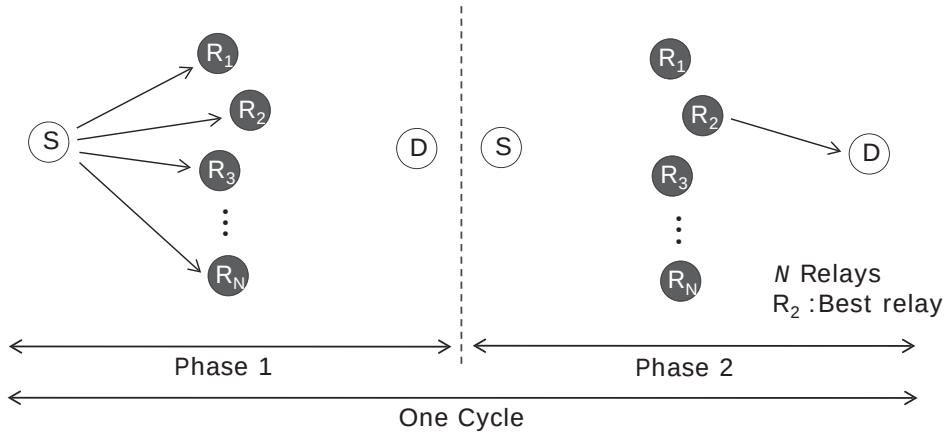

Figure 2.2: Example of opportunistic DF communication

reactive relay selection. The reactive relay selection excludes the relays that did not decode the source data, thus, the relay selection complexity can be decreased while preserving the performance.

Since the wireless medium is a shared resource, controlling channel access is crucial in determining the throughput of the wireless network and has an impact on system complexity. The MAC layer controls how different users share the given spectrum and ensures reliable data transmissions. As a medium access protocol, we adopt carrier sense multiple access with collision avoidance (CSMA/CA), which reduces the number of collisions by an exchange of control packets called RTS and CTS packets. Given the system model, the MAC layer transmission sequences are illustrated in Fig. 2.3. The transmitted signals and the received signals of each node are represented as a solid box and a dotted box, respectively. If the wireless medium is continually idle for a DIFS duration, the source initiates communication by transmitting RTS. Once the destination receives the RTS, it transmits a CTS to the source. Relays within the range of the RTS and CTS signals can estimate their channel gains by listening to those signals. We assume that the RTS and CTS packets can be successfully received at the destination and the source, respectively. However, the actual data packets use relays to communicate with the destination. This assumption can be easily justified

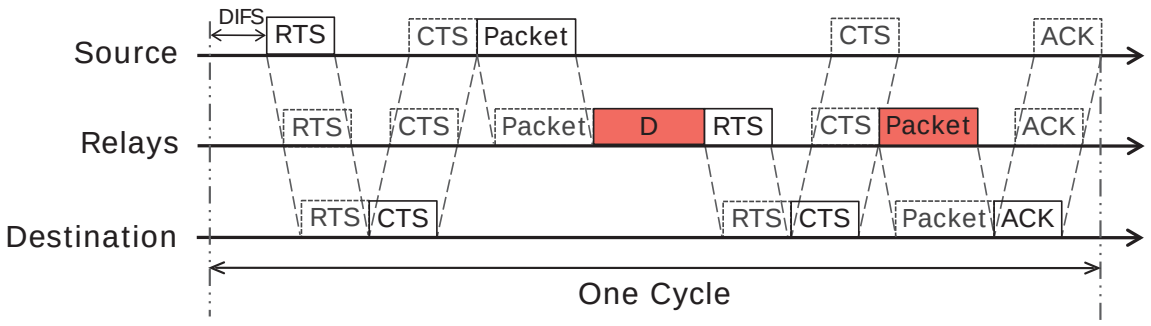

Figure 2.3: MAC layer relay transmission sequences

if the rate for the RTS/CTS frames is small. The source transmits the data packet to the relays and the relay selection is executed among the relays that successfully decode the source data. We denote the average time for relay selection as D (see Fig. 2.3). The selected relay sends RTS packet to the destination which indicates to the source and all the other relays that a relay is chosen. The destination transmits CTS frames to avoid a collision when the data is transmitted from the relay to the destination. Then the relay forwards the data packet to the destination. If the destination decodes the relayed data successfully it transmits an acknowledgement (ACK) back to the relay. We define this procedure as one cycle. In this system model, it is assumed that the relays do not communicate their channel gains with one another. Thus, the relay only has its own channel gain information toward source and destination, respectively. Using this distributed channel gain information, the relay selection is performed, where the details of the relay selection method will be addressed in Section 5.2.2.

2.4.2 Outage Probability Analysis

In multiple-relay networks, the outage probability is affected by the number of relays available in the network and the cooperation protocol used. In this section, we define the optimal relay in terms of minimizing the outage probability for relays with single

antenna and multiple antennas. Efforts have been made to find the optimal relay set or antenna set which achieves maximum diversity gain [11] [46]. However, in our system and channel model, it is sufficient to choose a single best relay to achieve the maximum diversity order as in [46]. This is because the outage probability (2.23) does not depend on the fast fading channel realization, only its statistical characteristics and the shadow fading level. In addition, since the diversity gain depends on the minimum number of antennas between the transmitter and the receiver [47], if all the nodes have the same number of antennas, cooperating with a single best relay is optimal in terms of diversity gain, in our communication model.

Suppose the source and the selected relay are transmitting at the same rate R (in bits/s/Hz), where we assume equal time duration for the source and the relay transmission. We further assume that all the relays are clustered at the midpoint between the source and destination, and their distance from each other is negligible when compared to the distance from the source and the destination. Under this assumption, if relay i is used in the communication, an end-to-end outage is said to occur if the minimum of the capacity of the source to relay i and the capacity of relay i to destination link is less than R as follows

$$\min\{C(L_{Si}), C(L_{iD})\} < R,$$

where L_{Si} and L_{iD} are the lognormal random variables representing the shadowing between the source to relay i and the relay i to destination, respectively. We assume that each of the relays experiences independent shadowing, and L_{Si} and L_{iD} are also independent. Thus, in a proactive relay selection, the shadowing level for the optimal relay, I_p is the maximum shadowing level of the minimum shadowing level of the

source-to-relay and relay-to-destination links as follows

$$I_p = \arg \max_{i=1,..,N} \min(L_{Si}, L_{iD}).$$

Since the capacity function $C(\cdot)$ is a monotonic increasing function of the shadow fading level, the optimal relay I_p is obtained by comparing each relay's shadow fading levels. The corresponding outage probability is given by

$$\begin{aligned} P_{out}(R) &= Pr\left(\max_{i=1,..,N} \{\min\left(C(L_{Si}), C(L_{iD})\right)\} < R\right) \\ &= Pr\left(\max_{i=1,..,N} \{\min\left(L_{Si}, L_{iD}\right)\} < g(R)\right) \\ &= \prod_{i=1}^{N} \{1 - Pr\left(L_{Si} > g(R)\right) Pr\left(L_{iD} > g(R)\right)\} \\ &= \prod_{i=1}^{N} \left\{1 - Q\left(\frac{\ln(g(R))}{\sigma_{Si}}\right) Q\left(\frac{\ln(g(R))}{\sigma_{iD}}\right)\right\}, \end{aligned} \tag{2.24}$$

where σ_{Si} and σ_{iD} are the standard deviations of the normal random variables corresponding to the log normal shadowing. For mathematical simplicity, we consider the symmetric scenario where the distribution of the shadow fading of the source to relay and the relay to destination are identical. Then, the outage probability (2.24) can be written as

$$P_{out}(R) = \left\{1 - Q\left(\frac{\ln(g(R))}{\sigma}\right)^2\right\}^N, \tag{2.25}$$

where $\sigma = \sigma_{Si} = \sigma_{iD}$. This outage probability expression incorporates the effects of the shadow fading characteristics and the number of available relays on outage probability. Note that the outage probability decreases as the number of available relays increases or as the variance of the lognormal shadowing increases.

Now consider a reactive relay selection, in which the relay selection is performed after the source transmission of the data. The optimal relay, I_r has the maximum

channel gain from the relay to destination among the relays that successfully decode the source data. Suppose $\mathcal{M}$ is the set of relays that successfully decode the source data, and has size $|\mathcal{M}| = \mathcal{D}$. Then the optimal relay is defined as follows

$$I_r = \arg\max_{i \in \mathcal{M}} L_{iD}. \tag{2.26}$$

The relay chosen in reactive selection can be different from the relay chosen in proactive selection. Consider a network with two relays: relay 1 and 2. If both relays decode the source data successfully, they are in the set $\mathcal{M}$, and their shadowing levels are as follows

$$L_{S2} < L_{S1} < L_{1D} < L_{2D},$$

then relay 1 is chosen in the proactive selection. On the other hand, relay 2 is chosen in the reactive selection because relay 2 has the maximum shadowing level from the relay to destination link. However, their outage probability remains the same if the transmission rates of the source-to-relay and the relay-to-destination are the same. The analytical proof of this observation follows below. In the reactive relay selection, the corresponding outage probability is given by

$$P_{out}(R) = \sum_{n=0}^{N} Pr(\max_{i \in \mathcal{M}} C(L_{iD}) < R | \mathcal{D} = n) Pr(\mathcal{D} = n) \tag{2.27}$$

The cardinality probability $Pr(\mathcal{D} = n)$ in (2.27) has a binomial distribution as follows

$$\begin{aligned} Pr(\mathcal{D} = n) &= \binom{N}{n} Q\left(\frac{\ln(g(R))}{\sigma}\right)^n \left(1 - Q\left(\frac{\ln(g(R))}{\sigma}\right)\right)^{N-n} \\ &= \binom{N}{n} \mathcal{Q}^n (1 - \mathcal{Q})^{N-n}, \end{aligned} \tag{2.28}$$

where

$$\mathcal{Q} = Q\left(\frac{\ln(g(R))}{\sigma}\right). \tag{2.29}$$

Using (2.28), the outage probability (2.27) becomes as follows

$$\begin{aligned} P_{out}(R) &= \sum_{n=0}^{N} (1-\mathcal{Q})^n \binom{N}{n} \mathcal{Q}^n (1-\mathcal{Q})^{N-n} \\ &= (1-\mathcal{Q})^N \sum_{n=0}^{N} \binom{N}{n} \mathcal{Q}^n \\ &= (1-\mathcal{Q}^2)^N, \end{aligned}$$

which is equal to the proactive outage probability derived as (2.25). This verifies that the reactive relay selection method has the same outage probability as the proactive relay selection, but has lower selection complexity.

2.5 Numerical Results

In this section the opportunistic relay communication outage probability in terms of the received SNR, γ is evaluated. For the following results, we assume that the source to destination distance is 1 km, the path loss exponent η is 3, the mean and the variance of lognormal shadowing are 0 and 10 dB respectively, and the transmission SNR is fixed as $\gamma \times (d/2)^2$ dB, where d is the distance between the source and the destination.

Fig. 2.4 shows the outage probability comparison between the point-to-point communication and the relay communication where the number of relays, N, is 5. The target end-to-end rate R is 1 bits/s/Hz; thus, the corresponding relay communication single hop target rate is 2 bits/s/Hz. The figure shows that the relay communication has the merit of achieving a lower outage probability at the same end-to-end rate. Furthermore, it is also shown that the outage probability using the high SNR approximation of capacity $\widetilde{f}(L)$ almost perfectly matches the exact evaluation of the outage probability not only in the high SNR regime but also in the low SNR regime. This is because the disregarded high order terms decay as long as γ is greater than 1, which

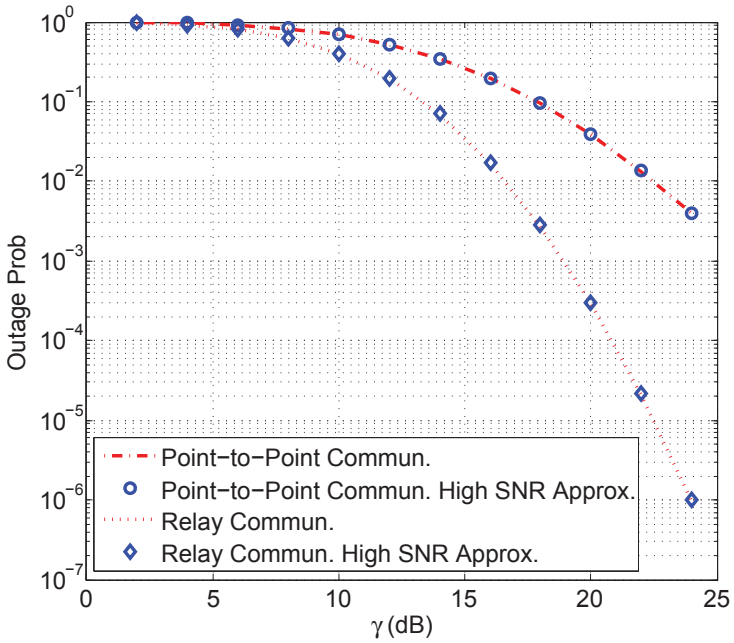

Figure 2.4: Comparison between point-to-point and relay communication

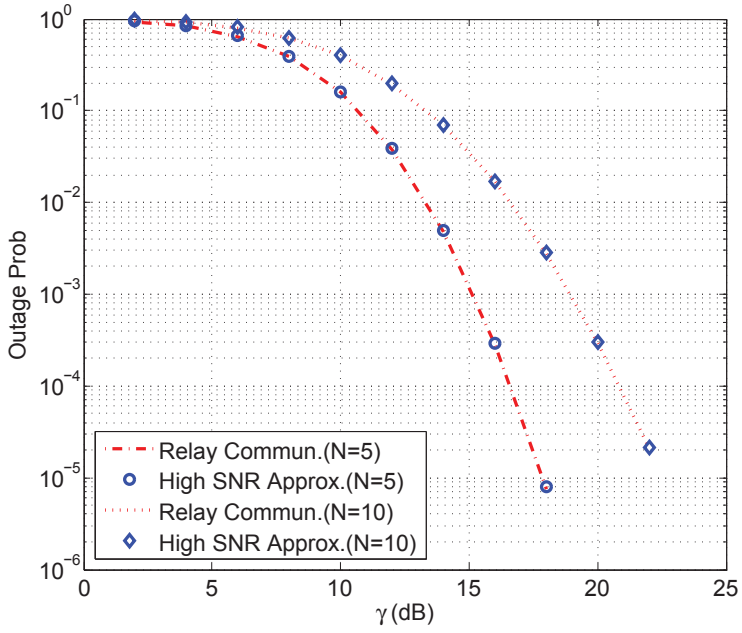

Figure 2.5: Outage probability in terms of different number of relays

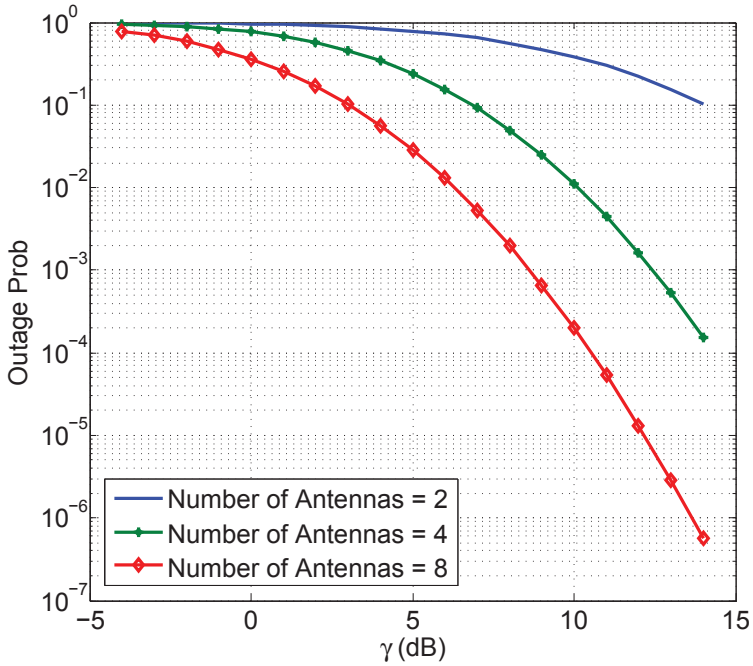

Figure 2.6: MIMO relaying outage probability with different number of antennas

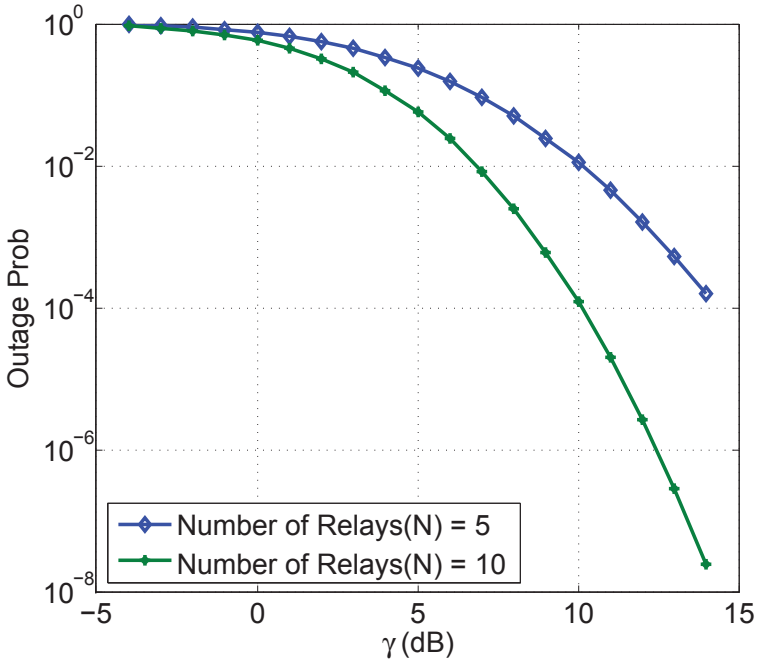

Figure 2.7: MIMO relay network outage probability in terms of different number of relays

is a 0 dB received signal. The outage probability of opportunistic relay communication with respect to the average received power for the different number of relays in the network is shown in the Fig. 2.5. If the number of relays is doubled, from 5 to 10, the SNR gain is slightly greater 3 dB at an outage probability of 10^{-4}, which is anticipated because the diversity order is increased by factor of 2 if the number of relays is doubled.

Fig. 2.6 shows the outage probability of the opportunistic MIMO relay communication with different number of antennas versus the average received SNR, where the target end-to-end rate is 4 bits/s/Hz, and the number of relays is 5. It is obvious that the outage probability decays as the number of antennas and the SNR increases. For example, to achieve the outage probability of 10^{-4}, the network with 4-antenna nodes requires more than 3 dB SNR than the network with 8-antenna nodes. This is because the diversity order of the network increases as the number of antennas at each node increases. As in single antenna network, the diversity order also increases as the number of relays in the network increases, which is shown in Fig. 2.7, where the number of antennas is 4. To achieve the outage probability of 10^{-4}, the network with 5 relays requires more than 3 dB SNR than the network with 10 relays. This is also expected result since the diversity order of the network with 5 relays of 4-antenna, and a network with 10 relays of 8-antenna is the same.

2.6 Conclusion and Future Research

In this chapter we have studied opportunistic relay communication for two-hop decode and forward networks, in particular, by finding the outage probability for mixed channel effects. When fast fading and slow fading are assumed, the Shannon capacity is no longer a suitable performance criterion since it does not effectively provide the rate limit information which is possible over a given and arbitrary block of data. This is why we evaluated outage probability, and we found that the outage probability de-

pends on the shadow fading characteristics. Based on these findings, we evaluated an outage probability in a single antenna network and also for a multiple antenna network. We further evaluated the outage probability of an opportunistic relay network. We found that the outage probability of the relay network also depends on the shadow fading characteristics of each hop link, and it is simply derived as a Q-function polynomial.

Currently we assumed all relays are located in the mid-point between the source and destination, and we also assumed that the shadow fading gains of each relays are independent. However, since shadow fading depends on the topographical circumstance, relays could have correlated shadow fading gains. In this scenario, the end-to-end outage probability might not be simplified as a Q-function polynomial. It will be interesting to investigate the outage probability of the correlated shadow fading gains between each relays.

The analysis of the opportunistic cooperative channels studied in this chapter can be further extended by considering the overhead of a MAC layer control signal, which motivates the need for cross-layer design and its performance analysis. In the next chapter, we will study the MAC layer relay selection protocol and evaluate its impact on the relay selection period.

CHAPTER III

Opportunistic Relay Selection and Selection Period

3.1 Introduction

There are fundamental engineering principles that need to be understood in order to design relay networks. These fundamental engineering principles, however, need to be relevant to practical system design. A typical communication system has multiple design layers. At the lowest layer is the physical layer. The physical layer provides transmission of information and includes the modulation and coding. The next layer is the MAC layer. The MAC layer uses the physical layer in order to coordinate transmission of information between different nodes in the network. The next layer is the network layer which determines how a packet should be routed through a network. In a multi-relay network, which relay or relays a network should employ in communicating information between a source and a destination has to be determined. This decision cannot be solely determined by studying the physical layer, but it must also depend on the protocol used in the other layers. For instance, the MAC layer can assign a longer channel usage time to users with low-rate modulation schemes to meet a throughput constraint; the network layer can reroute traffic to links supporting high-rate modulation schemes to minimize congestion; and the application layer can

use coding schemes to leverage the diversity of different routes. Therefore, designing and understanding the physical layer protocols jointly with the protocols of the upper layers is needed.

In opportunistic relay communications, relay selection is based on the maximum of a relay signal strength metric, which is the minimum signal strength between the source to relay and the relay to destination, where the required CSI can be obtained by listening to MAC layer control signals such as an RTS and a CTS. Given that RTS/CTS is already incorporated in most MAC protocols and needed anyway, an opportunistic relay communication and the relay selection needs to be optimized considering the MAC layer overhead. This chapter discusses the optimization of the timer based relay selection protocol in terms of minimizing relay selection time. Incorporating the MAC layer overhead of an opportunistic relay communication, we find the throughput maximizing relay selection period.

3.2 Relay Selection Protocol

3.2.1 Distributed Timer Algorithm [10]

In the previous chapter, which relay to select in a multi-relay network is addressed. In addition, how the relay is selected is also important factor that affects the actual system throughput because selecting a relay requires additional system resources compared to using a fixed relay. According to the distributed timer algorithm, after the relays obtain their channel gains, the relays that successfully decode the source data set their timers inversely proportional to the channel gain from them to the destination. For the channel model that we are considering, the initial timer value of relay i, denoted by Ω_i, can be set according to the shadow fading level as follows

$$\Omega_i = \kappa \frac{1}{L_{iD}}, \tag{3.1}$$

where κ is the timer scaling factor. The relay that has the highest shadowing level, thus has the minimum Ω_i, expires first and sends an RTS packet to the destination. We assume that each relay is in the listening state when its timer is running. A collision occurs when the differences between initial timer values of the relay with minimum Ω_i and the next smallest Ω_j is less than the propagation delay between those relays plus a short interframe space (SIFS). Thus, the collision probability will depend on the scaling factor κ, and the number of relays in the network, N. For instance, as N increases, the collision probability increases. To reduce the collision probability, one can increase κ to make larger differences in initial timer values. However, this increases the relay selection time proportionally. Thus, κ should be carefully chosen to reduce the collision probability, and at the same time, minimize the selection time.

3.2.2 Analysis of Average Relay Selection Time

In this section, we analyze the average relay selection time of the distributed timer algorithm. We also find the optimal timer scaling factor that minimizes the average relay selection time, and suggest a collision resolving mechanism in the relay selection phase. The reason for selecting the optimal relay, not just a relay that has the sufficient channel gain, is the fact that the optimal relay will be able to decode and forward the data for a longer time duration than a relay chosen that has sufficient channel gain, if the correlation of each of the shadow fading is the same. Thus, the selection is required less often. This will be addressed in detail in Section 3.3.

Suppose the summation of the propagation delay between the relay with minimum Ω_i and the next smallest Ω_j, and the SIFS is τ_p, then the collision probability $P_c(\kappa)$ can be defined as follows

$$P_c(\kappa) = \sum_{n=0}^{N} Pr(\min_{i \neq I, i \in \mathcal{M}} \Omega_i - \Omega_I < \tau_p | \mathcal{D} = n) Pr(\mathcal{D} = n). \tag{3.2}$$

For notational convenience, we denote the optimal relay chosen by the reactive relay selection algorithm I_r in (2.26) as I, and we will denote L_{iD} as L_i in the following analysis. The conditional collision probability in (3.2) can be determined as

$$\begin{aligned}
&Pr(\min_{i\neq I, i\in\mathcal{M}} \Omega_i - \Omega_I < \tau_p | \mathcal{D} = n) \\
&\quad = Pr(\min_{i\neq I, i\in\mathcal{M}} \frac{1}{L_i} < \tau_p/\kappa + \frac{1}{L_I} | \mathcal{D} = n) \\
&\quad = 1 - \sum_{j\in\mathcal{M}} Pr(\min_{i\neq I, i\in\mathcal{M}} \frac{1}{L_i} > \tau_p/\kappa + \frac{1}{L_I}, I = j | \mathcal{D} = n) \\
&\quad = 1 - \sum_{j\in\mathcal{M}} Pr(\max_{i\neq j, i\in\mathcal{M}} L_i < \frac{L_j}{L_j\tau_p/\kappa + 1}, \max_{i\neq j, i\in\mathcal{M}} L_i < L_j | \mathcal{D} = n) \\
&\quad = 1 - \sum_{j\in\mathcal{M}} \int_0^\infty Pr(\max_{i\neq j, i\in\mathcal{M}} \Gamma_i < \ln \frac{x}{x\tau_p/\kappa + 1} | \mathcal{D} = n, L_j = x) f_{L_j}(x) dx \\
&\quad = 1 - n \int_0^\infty \left(1 - Q\left(\frac{\ln \frac{x}{x\tau_p/\kappa+1}}{\sigma}\right)\right)^{n-1} f_{L_j}(x) dx.
\end{aligned}$$

This shows that as σ increases or κ decreases, $P_c(\kappa)$ increases, which means there is a tradeoff between the relay selection time and the collision probability. We denote the selection time without a collision as D_1 and the extra average time required to resolve the collision as D_2. Then the average relay selection time, denoted by D can be found as follows

$$\begin{aligned}
D &= \min_\kappa (1 - P_c(\kappa)) D_1 + P_c(\kappa)(D_1 + D_2) \\
&= \min_\kappa D_1 + P_c(\kappa) D_2. \qquad (3.3)
\end{aligned}$$

The selection time without a collision D_1 is determined as follows

$$D_1 = E\left[\kappa \frac{1}{L_I}\right],$$

where the cumulative distribution function of $1/L_I$ can be found as follows

$$\begin{aligned} Pr(1/L_I < x) &= Pr(1/x < L_I) \\ &= 1 - \left(1 - Q\left(\frac{-\ln x}{\sigma}\right)\right)^N. \end{aligned}$$

Thus, the expectation of $1/L_I$ can be obtained as follows

$$\begin{aligned} E\left[\frac{1}{L_I}\right] &= \int_0^\infty 1 - Pr(1/L_I < x)dx \\ &= \int_0^\infty \left(1 - Q\left(\frac{-\ln x}{\sigma}\right)\right)^N dx. \end{aligned}$$

The average selection time when a collision occurs depends on how the collision is resolved. One can increase the scaling factor κ to make larger differences in the timer setting. However, even for a large κ, if the channel gain difference is small, a collision can still occur. Further, it will be a waste of resources to figure out the optimal relay if there is only a negligible difference between the channel gains of the optimal relay and the second-best optimal relay. In addition, if there are more than two relays which have initial timer values less than τ_p, a collision is not avoidable. Thus, we propose two collision resolving-phases: increasing κ in the resolving-phase 1, and random selection in the resolving-phase 2.

In the resolving-phase 1, we suggest to increase κ to κ' which makes the initial timer value less than τ_p for the relays with the higher fading level than a certain fading level threshold. This threshold L_T, for example, can be determined by the shadow fading level that has 3 dB higher value than the value that achieves the target rate. Then the corresponding scaling factor can be determined by finding κ' that satisfies

$$\kappa' \frac{1}{L_T} = \tau_p.$$

Then, if a collision occurs again, in the resolving-phase 2, a relay is chosen randomly among the relays involved in the collision. Without the resolving-phase 1, D_2 in (3.3) becomes the average time of the random relay selection. In this case, if the random selection requires a smaller amount of time than the distributed timer selection ($D_2 << D_1$), then a relatively small κ (large $P_c(\kappa)$) becomes the solution for (3.3), and the probability of a random selection increases. Thus, we need the resolving-phase 1 to reduce the suboptimal relay selection probability.

For the aforementioned collision resolving mechanism, the time requirement D_2 becomes as follows

$$\begin{aligned} D_2 &= D_3(1 - P_c(\kappa')) + (D_3 + D_4)P_c(\kappa') \\ &= D_3 + D_4 P_c(\kappa'), \end{aligned} \tag{3.4}$$

where D_3 is the average selection time without a further collision, and D_4 is the extra time requirement for resolving a second collision, which is a required time for random selection. We define τ_p' as the back off time for the relay to find out that a collision occurred, which includes the propagation delay between the source and relays, slot time, and the short interframe space (SIFS). Then, we can find D_3 as follows

$$D_3 = \tau_p' + \kappa' E\left[\frac{1}{L_I}\right].$$

The random timer setting method is the same as the random backoff timers of IEEE 802.11 standard, which guarantees no collision in the random selection. We assume that the relays involved in the collision know there was a collision. This assumption is reasonable if the relays are capable of listening to other signals while their timer is running. We further assume that each relay has its own index from 1 to N obtained by assigning an index at the very beginning of the communication. Thus, in the resolving-phase 2, the relays involved in the collision set their timers according

to their indices such as $\tau_{ST}n$, where τ_{ST} is the slot time (minimum window size) and n is the index ($n = 1, 2, ..., N$). Then the extra time requirement D_4 becomes as follows

$$D_4 = \tau_p' + \tau_{ST}\frac{N+1}{2}.$$

By substituting (3.4) into (3.3), the average relay selection time becomes as follows

$$D = \min_{\kappa} D_1 + P_c(\kappa)(D_3 + P_c(\kappa')D_4).$$

Note that D depends on the number of relay candidates N. As κ increases, the first term D_1 increases monotonically and the second term related to $P_c(\kappa)$ decreases monotonically. Therefore, there exist optimal κ that minimizes the average selection time, which can be found numerically.

3.3 Optimal Relay Selection Period

By setting an optimal scaling factor, average relay selection time can be minimized. However, selecting the optimal relay requires time resources and this additional time can decrease the overall throughput. In the channel model that we are considering, if the shadowing is highly correlated across codewords, once the optimal relay is selected, it is likely to be selected in the following transmission cycle. In this case, executing the selection algorithm at every cycle will degrade the throughput. In addition, even if the selected optimal relay does not remain optimal in the following transmission cycle, if the channel gain difference is small; using the previously chosen relay is optimal in the sense of throughput. These observations indicate there is an optimal cycle for the relay selection.

The status of the optimality of the selected relay depends on the shadow fading dynamics. The shadow fading dynamics are described by the autocorrelation function

of the lognormal shadow fading process. The autocorrelation function depends on the velocity of a mobile node. Thus, the optimal relay selection period will vary according to the velocity of nodes. Suppose T denotes the relay selection period which means the relay selection is executed every T cycles. We denote the index of cycle within the period as m. When $m = 1$, the optimal relay selection is performed and for $m = 2, ..., T$, the relay chosen at $m = 1$, $I(1)$ is used without running the relay selection algorithm. Thus, when $m \neq 1$, transmission is done via a potentially suboptimal relay but in return, resources used for selection are saved.

Suppose A denotes the number of transmitted bits in one cycle. Let X_m be a r.v. measuring the number of successfully received bits at the destination at cycle m. The throughput of the system with the selection period T, denoted by $S_T(v)$, is given by

$$S_T(v) = \frac{\sum_{m=1}^{T} E[X_m]}{D + \tau T}, \tag{3.5}$$

where τ is the time duration of one cycle without the relay selection phase, and $E[X_m] = E[E[X_m|\mathcal{M}]$. The expected number of bits $E[X_m]$ successfully received at the destination is a function of the autocorrelation function $\rho((m-1)\tau)$. When $m \neq 1$ (the proof can be found in appendix):

$$E[X_m] = AN \int_{-\infty}^{\infty} Q\left(\frac{\ln(g(R)) - \rho((m-1)\tau)x}{\sqrt{(1-\rho((m-1)\tau)^2)\sigma^2}}\right)\left(1 - Q\left(\frac{x}{\sigma}\right)\right)^{N-1} f_{\Gamma_1}(x)dx.$$

Since the autocorrelation function is a function of v, $E[X_m]$ and the throughput $S_T(v)$ are also functions of v. Then the optimal selection period, which maximizes the system throughput, denoted by $T^*(v)$, is given by

$$T^*(v) = \arg\max_{T}(S_T(v)), \tag{3.6}$$

where the system throughput incorporating the optimal selection period can be found

by using (3.6) in (3.5). The analysis of the system throughput in terms of the selection period will be addressed in the next section.

3.4 Numerical Results

In this section we present numerical results of the opportunistic relay communication outage probability in terms of the received SNR, which is defined in the right hand side of (2.16). For the following results, we set the source to destination distance as 1 km, the number of relays N as 10, and the path loss exponent η as 3. The mean and the variance of lognormal shadowing are 0 and 10 dB, respectively. We assume that all relays are clustered at the midpoint of the source and destination.

Fig. 3.1 shows the collision probability with respect to the scaling factor κ, where κ is normalized by 10^{-6}. The figure indicates that to achieve a collision probability of 0.05, the normalized timer scaling factor increases from 5 to 13, as the number of relays increases from 10 to 30. Proportional to the scaling factor, the average relay selection time without a collision, D_1 increases, but the collision probability does not decrease proportionally. This is because the initial timer decreases slower in the high SNR region, thus increasing the scaling factor does not increase differences of the initial timer value as much as in the low SNR region.

The average relay selection time using the optimal scaling factor as a function of the number of relays is shown in Fig. 3.2. In these results, the back off time τ_p' is 79 μs, which is the summation of slot time τ_{ST} as 50 μs, SIFS as 28μs, and the propagation delay as 1 μs. The threshold level of the shadow fading is set as 3 dB higher than the shadow fading level that achieves the target rate. The average relay selection time increases as the number of relays increases, but the increment rate decreases. This is because the collision probability increases in the network with a large number of relays, and the average time for the collision resolving mechanism is deterministic.

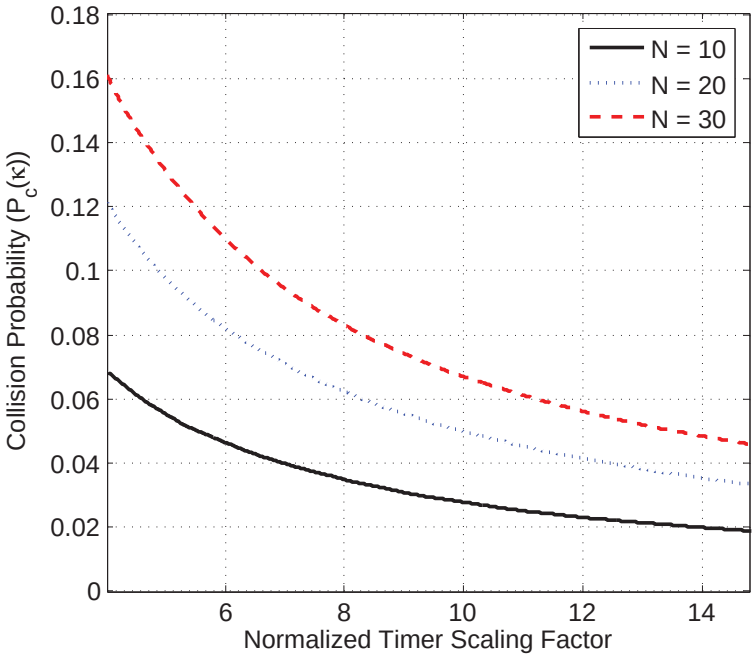

Figure 3.1: Collision probability of the relay selection with respect to κ

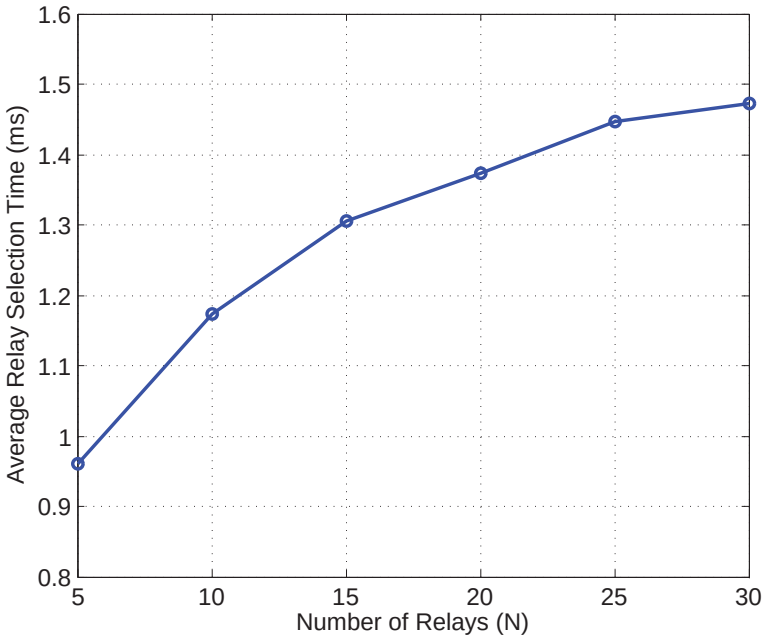

Figure 3.2: Average relay selection time versus the number of relays

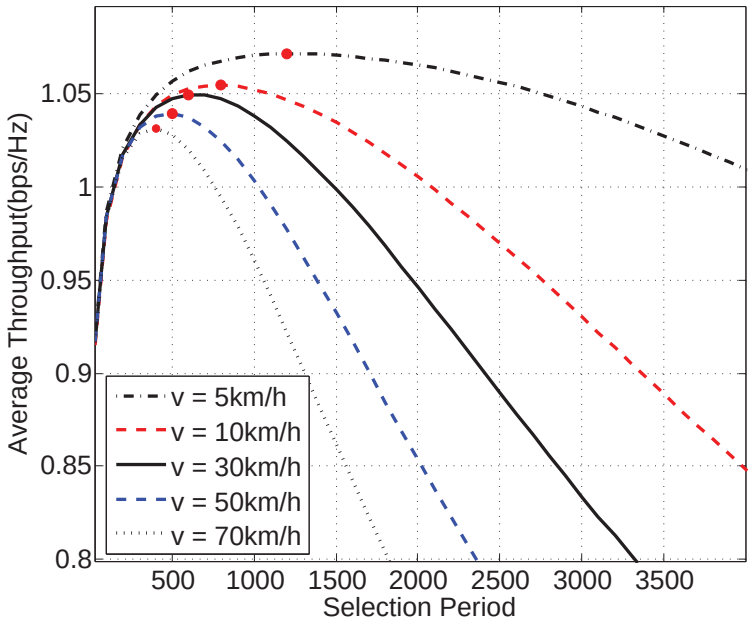

Figure 3.3: System throughput with respect to the selection period

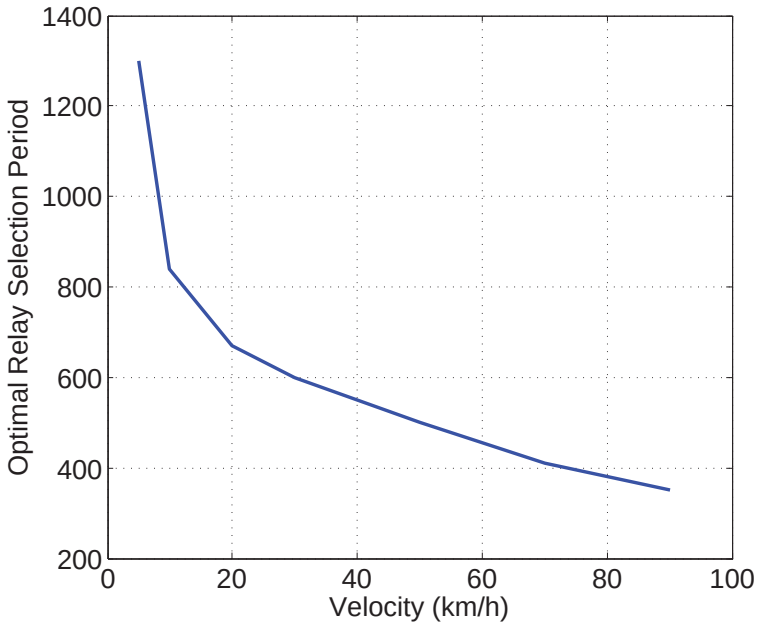

Figure 3.4: The optimal relay selection period with respect to the velocity of a mobile node

Fig. 3.3 shows the numerical result of the throughput with different periods and velocities. In this analysis, we assume the number of relays N is 5. We find the corresponding average relay selection time for this case is 965 μs. The correlation parameter ϵ_d is 0.15, and the SNR is 18 dB. The marked points represent the throughput maximizing selection period. We observe that if we select the optimal relay at every cycle (or very often), the throughput does not depend on the vehicle velocity, but it is less than the throughput of the optimal selection period. However, more importantly, the throughput difference between the velocity of 5 km/h and 70 km/h is less than 1 %. In other words, if the relay selection is executed in optimal period, the system throughput remains close to the optimal even the velocity of a mobile node increases. Fig. 3.4 also shows that as the velocity of a vehicle increases, the optimal relay selection period decreases. Fig. 3.4 shows the dependence of the optimal relay selection period on velocity. The decrease in the optimal relay selection period with increasing velocity is due to the exponential dependence of the shadowing correlation on velocity.

3.5 Conclusion and Future Research

In this chapter, we treated in detail the opportunistic relay selection protocol. We have investigated the relay selection and the selection period to connect the physical layer analysis to the MAC layer. We have shown that the distributed timer relay selection algorithm can incur collision in the selection phase, and the collision probability depends on the initial scaling factor of the distributed timers. Based on the analysis of the collision probability, we found the average relay selection time is a convex function of the timer scaling factor, thus there exists a timer scaling factor that minimize the average relay selection time. We further analyzed the effects of fast and slow fading in the relay selection protocol in terms of maximizing throughput. The observation that the shadowing is a time-correlated random process allows the

relay selection to be executed in a certain interval of packet transmissions. We found out that the overall throughput of the relay communication system is not degraded by the mobility of nodes if the relay selection is performed in the optimal selection period.

This chapter addressed the challenges in relay communications with homogeneous nodes, where all nodes have an equal number of antennas. Relaying with a single best relay is optimal under this condition. However, if the relays have different number of antenna, we have to consider an antenna selection scheme or choose multiple relays. We are planning to develop this MIMO relay analysis with heterogeneous nodes and find an opportunistic scheme that maximizes diversity of the network. Another research problem worth considering is to consider different detection schemes such as minimum mean square error (MMSE) estimation or zero forcing, where the transmitter node does not require CSI. Comparing the throughput between the transmitter beamforming scheme and the MMSE estimation scheme incorporating MAC layer overhead will be considered in the future research.

CHAPTER IV

Throughput Analysis of Multi-hop relaying: the Optimal Rate and the Optimal Number of Hops

4.1 Introduction

A natural extension of a single relay two-hop communication network is a multi-hop relay network. By dividing a path into a set of shorter hops, multi-hop transmission can lead to power reduction compared with direct transmission. Multi-hop wireless networks have far ranging practical applications. Monitoring infrastructure is one such application. Deteriorating bridges require monitoring the health of bridges to avoid future disasters. In monitoring bridges sensors are deployed on the steel beams that measure vibration and detect structural cracks before a disaster occurs. These sensors are distributed over the bridge and the data must be communicated with a central station where the data is collected, processed and analyzed. Long lifetime nodes are required since replacing a battery in a node might involve shutting down the roadway (either below the bridge or on the bridge) or at least deploying a crew for this purpose. Multi-hop networks are a viable alternative since the propagation conditions from every sensor to the central collection station would likely require a significant amount of energy.

Multi-hop relay networks are able to exploit the dynamic path diversity by select-

ing the optimal path using the appropriate routing technique. Traditional routing techniques have the merit of network scalability and enhanced connectivity [26][36]. Multi-hop cooperative networks, in addition, harness the broadcasting transmission property of a wireless system in order to maximize end-to-end rate and to reduce the outage probability. There have been attempts to find an exact expression for the outage probability and the throughput of a multi-hop relay network. For instance, in [6][15], the outage probability is analyzed considering independent paths from the source to the destination. However, to fully exploit the path diversity of the network, a routing algorithm that considers all possible paths is needed. A routing strategy that takes into account all possible paths is studied in [18], in which, a lower and upper bound on the multi-hop outage probabilities are derived. However, the exact outage probability was not found.

From a system throughput perspective, it is better to allow some frame outages by increasing the rate rather than reducing outages by decreasing the system rate as proved in [1]. This means that the throughput is maximized by using the optimal rate. In multi-hop cooperative networks, the end-to-end throughput is influenced by the number of hops and the raw transmission rate. Efforts have been made to maximize the throughput by finding the optimal routing strategy. For instance, in [14], the throughput gain of a multi-hop network is found along with the optimal number of hops. However, the optimal number of hops is found based on simulation because the analytical performance is difficult to evaluate. The authors in [4] also investigated the optimal number of hops considering the end-to-end outage probability. However, the outage probability analysis is restricted to the system where there is one relay candidate at each hop. As such, a closed form expression for the optimal number of hops, incorporating the end-to-end throughput, needs to be addressed.

In this chapter, a detailed overview is presented on various aspects related to the design of relaying in multi-hop cellular networks with emphasis on the overall

throughput analysis. We first find an exact expression for the outage probability of a multi-hop relay communication incorporating all possible paths. The major contribution of the analysis is the fact that the outage probability does not depend on whether the relay selection is performed before or after the source transmission. We define the effective throughput based on the precise outage probability, which is the rate that used in the system multiplied by the outage probability. Since the outage probability depends on the adapted rate, there exists an optimal operating rate that maximizes the effective throughput. We derive an expression for the optimal operating rate, and further investigate the optimal number of hops that maximizes the throughput with respect to the source to destination distance.

4.2 System Model

4.2.1 Relay Communication System Model

We consider a half-duplex multi-hop decode-and-forward relay communication system. Fig. 4.1 shows an M-hop relay network configuration. The system is comprised of a source node S, a destination node D, and multiple relay clusters with multiple relays between them, where R_i^m is the i-th relay at the m-th hop. We assume that the total number of relay is fixed to N, and the available relays at each hop cluster is the same. Thus, in an M-hop relay network, the number of relays in each hop is

$$N_M = \frac{N}{M-1}. \tag{4.1}$$

We denote the total distance from the source and the destination as d, and assume that the relay clusters equally spaced with distance d/M along the line with the source and the destination. This cluster-based multi-hop relay network is formed by the known scheme proposed in [37], where the cooperative links are formed by request of a source node in ad hoc, decentralized fashion. This linear multi-hop relay model

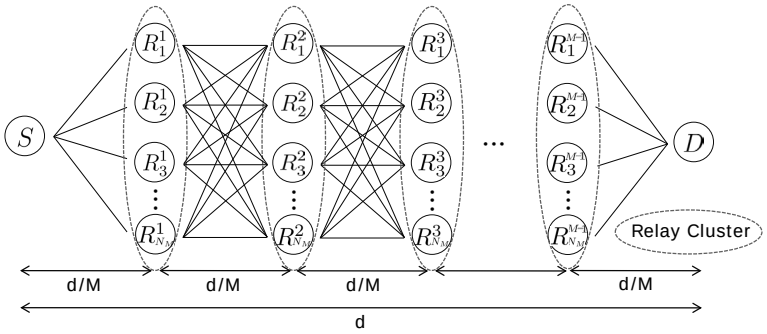

Figure 4.1: Example of an M-hop relay network topology

is commonly used for the analysis purpose [18] [6].

At any point of time, we assume that only one node is transmitting, thus there is no interference at any receiver. We also assume that only the neighboring relay clusters are in the range of transmission because of the power attenuation depends on the distance between the transmitter and the receiver. By this assumption, decoding at each node is executed based on the received signal from the neighboring transmitter relay. All the relays in each cluster can be a transmitter node for the next hop cluster and a receiver node for the previous hop cluster. Thus, the end-to-end path selection can be made by considering all the possible routing paths. In Fig. 4.1, for example, there exists $(N_3)^2$ possible paths, where some of paths are dependent.

We assume that a channel between any two-nodes is symmetric and the channel effects are perfectly known at the receiver. The transmitter has a statistical description of the fast fading, and knows the exact level of the shadow fading. The CSI is not shared with other relays. Using the local CSI, the relay selection is performed after the neighboring cluster's selected relay transmits data. By adopting this reactive relay selection, only the relays that correctly decode the forwarded data are considered as relay candidates for the next hop transmission, which reduces path selection complexity. Since the channel estimations for each link and the MAC layer overhead increases exponentially with the number of relay candidates, we only consider the reactive relay selection in this analysis.

4.2.2 Channel Model of a Single Hop Communication

As in the two-hop relay communications, the channel model considered takes into account path loss, shadowing, and fast fading effects. Given the channel model, the transmitted signal $x[k]$ and the received signal $y[k]$ in the neighboring hop relay can be related as follows

$$y[k] = \frac{h[k]\sqrt{L}}{(d/M)^{\frac{\eta}{2}}}\sqrt{\mathrm{E}}x[k] + w[k]. \qquad k = 1, ..., K \tag{4.2}$$

The difference between this multi-hop channel model and the direct communication channel model (2.1) is that the multi-hop communication has the path loss gain of M^η. The average received signal energy of a single hop, denoted by γ_M, can be written as

$$\gamma_M = E_{|h[k]|^2,L}\left[\frac{\mathrm{E}|h[k]|^2 L}{(d/M)^\eta}\right] = \frac{\mathrm{E}E[L]}{(d/M)^\eta} = \frac{\mathrm{E}E[L]M^\eta}{d^\eta},$$

where the direct communication received SNR can be found when $M = 1$. Using γ_M, the received signal (4.2) can be expressed as follows

$$y[k] = h[k]\sqrt{L\gamma_M}x[k] + w[k].$$

4.3 Multi-hop Relay Communication Performance Analysis

4.3.1 Outage Probability Analysis

In this section, a closed form expression for the multi-hop relay network throughput incorporating the system outage probability is derived. In an M-hop relay network, the achievable rate of a single link of the channel described in the previous section,

is found to be

$$C(L) = E_{|h|^2}\left\{\log\left(1+\frac{|h|^2 L\gamma_M}{N_0}\right)\right\} \tag{4.3}$$
$$= -\frac{e^{\frac{N_0}{L\gamma_M}}}{\ln 2} Ei\left(-\frac{N_0}{L\gamma_M}\right),$$

where the capacity is the function of the r.v. L and the received SNR γ_M. In each hop, an outage occurs when the target rate MR (in bps/Hz) in each hop is greater than the capacity (4.3). The corresponding single hop outage probability is given by

$$\begin{aligned} P_{out}(MR) &= Pr(C(L) < MR) \\ &= Pr\left(\Gamma < \ln\frac{g(MR)}{\gamma_M}\right) \\ &= 1 - Q\left(\ln\frac{g(MR)}{\gamma_M}\right) \\ &= 1 - \mathcal{Q}_M, \end{aligned} \tag{4.4}$$

where Γ is the log scale of the lognormal shadowing gain L, and $g(R)$ is the inverse function of the capacity (4.3). For our future use, we denote the Q-function in (4.4) as $\mathcal{Q}_M$, which is the successful transmission probability of a single hop in an M-hop relay network.

The number of possible paths for the M-hop relay network is N_M^{M-1}. In multi-hop relay network, an end-to-end outage occurs when all possible paths are in outage. Thus, the outage probability can be defined as follows

$$P_{out}(MR) = Pr\left(\max_{i=1,\ldots,N_M^{M-1}} \min\left\{C(L_{S,R_i^1}), C(L_{R_i^1,R_i^2}), \ldots C(L_{R_i^{M-1},D})\right\} < MR\right) \tag{4.5}$$

where the outage occurs when the largest minimum capacity is below the each hop target rate. In a 2-hop relay communication, deriving the end-to-end outage proba-

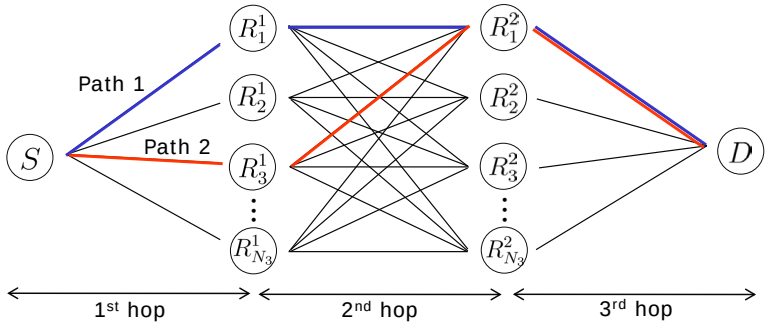

Figure 4.2: Example of 3-hop relay network paths

bility is relatively easy because all paths are independent. However, in a multi-hop relay network, a specific link may be shared by multiple paths. For instance, in a 3-hop relay network, as shown in Fig. 4.2, Path 1 and Path 2 shares the link from the second hop relay to the destination. Because of this dependency in paths, analysis has been restricted to the upper and the lower bound of the outage probability.

However, the exact outage probability can be derived by using the total probability. We focus on the fact that the reactive and the proactive relay selection achieves the same outage probability. In the multi-hop reactive relay selection, only the relays that correctly decode the forwarded data are considered in the relay candidates for the next hop. Suppose $\mathcal{M}_m$ is a set of the m-th hop relays that correctly decode the data, and has size $|\mathcal{M}_m| = \mathcal{D}_m$. Then paths from the relays in set $\mathcal{M}_m$ to the relays in the $(m+1)$-th relay cluster are considered in the selection and so on in the following hop. Using this reactive relay selection property and the law of total probability, we can find the end-to-end outage probability as follows

$$Pr(\mathcal{D}_m = p) = \sum_{q=0}^{N_M} Pr(\mathcal{D}_m = p|\mathcal{D}_{m-1} = q)Pr(\mathcal{D}_{m-1} = q). \tag{4.6}$$

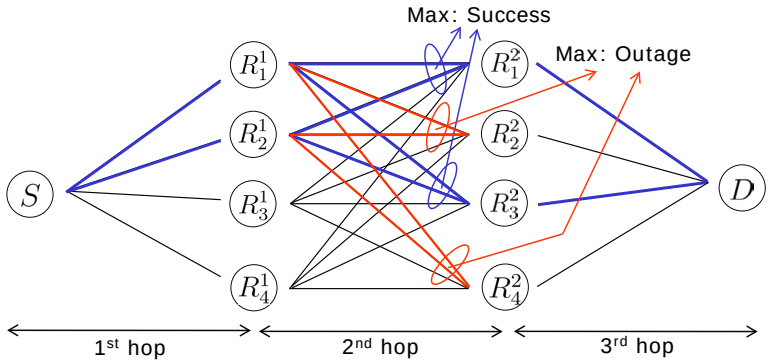

Figure 4.3: Example of a 3-hop relay network

The first hop cardinality probability has a binomial distribution as follows

$$Pr(\mathcal{D}_1 = p) = \binom{N_M}{p} \prod_{R_j^1 \in \mathcal{M}_1} Pr\left(C(L_{S,R_j^1}) > MR\right) \prod_{R_j^1 \notin \mathcal{M}_1} Pr\left(C(L_{S,R_j^1}) < MR\right)$$
$$= \binom{N_M}{p} \mathcal{Q}_M^p (1 - \mathcal{Q}_M)^{N_M - p}.$$

Since the reactive relay selection only considers relays that successfully decode the received data from the previous hop, by removing the path with outage from the selection candidate, the conditional probability of (4.6) can be derived. For instance, Fig. 4.3 shows a 3-hop relay network with 8 relays. If relay R_1^1 and R_2^1 decodes the data transmitted from the source successfully, in the link selection of the second hop, each relays in the second hop relay cluster finds the maximum channel gain link from the relay R_1^1 and R_2^1. If relay R_1^2 and R_3^2 have their maximum channel gains greater than the target rate, only the links that connected from those relays are considered in the next hop link selection. Thus, in general, the conditional probability can be found by

$$Pr(\mathcal{D}_m = p | \mathcal{D}_{m-1} = q)$$

$$= \binom{N_M}{p} \prod_{R_j^m \in \mathcal{M}_m} Pr\left(\max_{R_i^{m-1} \in \mathcal{M}_{m-1}} C(L_{R_i^{m-1}, R_j^m}) > R \right)$$
$$\times \prod_{R_j^m \notin \mathcal{M}_m} Pr\left(\max_{R_i^{m-1} \in \mathcal{M}_{m-1}} C(L_{R_i^{m-1}, R_j^m}) < R \right)$$
$$= \binom{N_M}{p} \left\{1 - (1 - \mathcal{Q}_M)^q\right\}^p \left\{(1 - \mathcal{Q}_M)^q\right\}^{N_M - p},$$

The outage probability of the last hop is defined as

$$Pr(\text{outage at the } M\text{-th hop} | \mathcal{D}_{M-1} = p) = Pr\left(\max_{R_i^{M-1} \in \mathcal{M}_{M-1}} C(L_{R_i^{M-1}, D}) < MR \right)$$
$$= (1 - \mathcal{Q}_M)^p.$$

4.3.2 The Optimal Rate and The Optimal Number of Hops

Due to the outage event, the effective throughput is less than the data rate in the absence of an outage. Incorporating the outage event, we define the throughput of the system $S(R)$ as

$$S(R) = (1 - P_{out}(MR))R. \tag{4.7}$$

For instance, the direct communication throughput can be expressed as

$$\begin{aligned} S(R) &= Pr(C(L) > R)R \\ &= Pr\left(\Gamma > \ln \frac{g(R)}{\gamma_1}\right) R \\ &= Q\left(\ln \frac{g(R)}{\gamma_1}\right) R \\ &= \mathcal{Q}_1 R. \end{aligned}$$

In (4.7), since the successful transmission probability, $1 - P_{out}(MR)$ is a concave function of R, the throughput is also a concave function. Therefore, we can find the

throughput maximizing rate by taking derivative as follows

$$\frac{dS(R)}{dR} = 1 - P_{out}(MR) - P'_{out}(MR)R.$$

Thus, the optimal rate of M-hop relaying R^* satisfies

$$R^* = \frac{1 - P_{out}(MR^*)}{P'_{out}(MR^*)}, \tag{4.8}$$

and the optimal number of hops M^* using the optimal rate is given by

$$M^* = \arg\max_M S(MR^*).$$

4.4 Numerical Results

In this section we first show the numerical analysis of the multi-hop relay network outage probability. Then, we find the throughput in terms of rate R and obtain the optimal rate with respect to the number of hops. Using the optimal rate, we also investigate the optimal number of hops when the source to destination distance d varies. For the following results, we set the number of relays N as 12, the path loss exponent η as 3, and the mean and the variance of the lognormal shadowing are 0 and 10 dB, respectively in a log scale.

Fig. 4.4 shows the outage probability comparison between the point-to-point communication and the multi-hop relay communication, where the number of hops varies from 1 to 4. The target end-to-end rate R is 1 bps/Hz, thus, for a M-hop relay network, each hop target rate is M bps/Hz. The distance d is 1 km, and the transmission SNR is fixed as $\gamma \times (d/2)^2$, thus, the x-axis is the received SNR of a two hop relay network. The figure shows that the relay communication has an advantage of low outage probability for the given number of hops. The figure shows that the

2-hop and 3-hop relay network outage probability achieves the outage probability of 10^{-3} for the γ of 14 dB. However, for the SNR below 14 dB, 3-hop relaying achieves the lower outage probability, and for the SNR above 14 dB, 2-hop relaying achieves the lower outage probability. This can be explained from the fact that capacity increases in log scale as the SNR increases, but the target rate increases linearly with the number of hops increases.

Fig. 4.5 and 4.6 shows the throughput versus the end-to-end rate, when γ is 12 dB. In this figure, the marked points represent the throughput maximizing rate. For the low rate regime, the slope of the throughput is R since the outage probability is close to zero (see the throughput expression (4.7)). As Fig. 4.4 shows, when γ is 12 dB, 3-hop relay performs better than the other relaying scheme, and Fig. 4.5 verifies this result. (See when the rate is 1 bps/Hz). However, it is also shown that the maximum throughput of the 3-hop relaying is achieved when the rate is 1.1 bps/Hz, and each multi-hop relaying scheme has different optimal rate that maximize the throughput. For instance, 2-hop relaying achieves its maximum throughput when the rate is 1.2 bps/Hz.

Fig. 4.6 shows the throughput with respect to the end-to-end rate when γ is 16 dB. When the end-to-end rate of 1 bps/Hz, it is shown in Fig. 4.4 that the 2-hop relaying achieves the minimum outage probability. However, Fig. 4.6 shows that the throughputs of the 2-hop and 3-hop relaying scheme are almost the same if the rate is 1 bps/Hz. The 2-hop relaying achieves its maximum throughput when the rate is 1.4 bps/Hz. Furthermore, when the each of relaying schemes adapts its optimal rate, we can see that the optimal number of hops for the given SNR is 2. This numerical analysis shows that rate adaption is necessary to make the most use of multi-hop relaying and find the optimal number of hops.

Fig. 4.7 shows the optimal number of hops in terms of the distance d for the relay network with and without buffers. In this analysis, we set the total number of relays

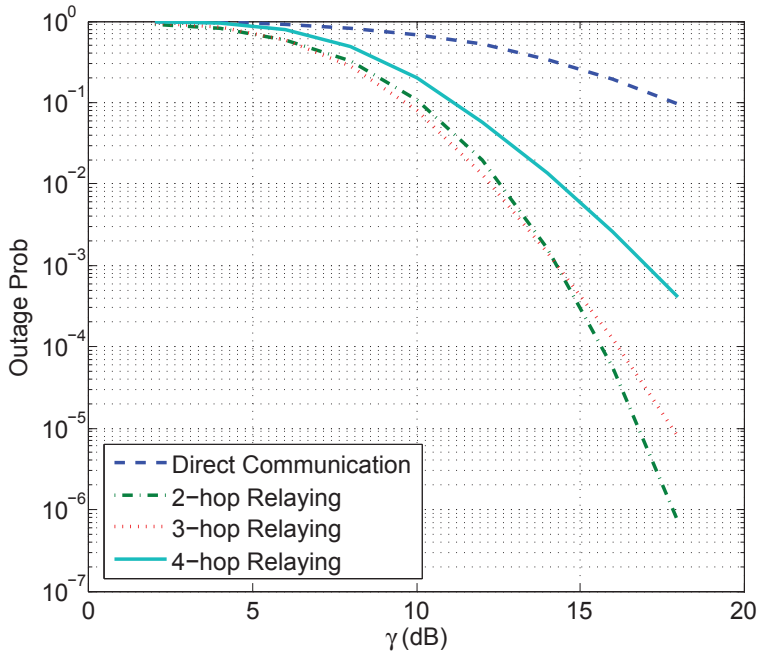

Figure 4.4: Outage probability analysis of a multi-hop relay network

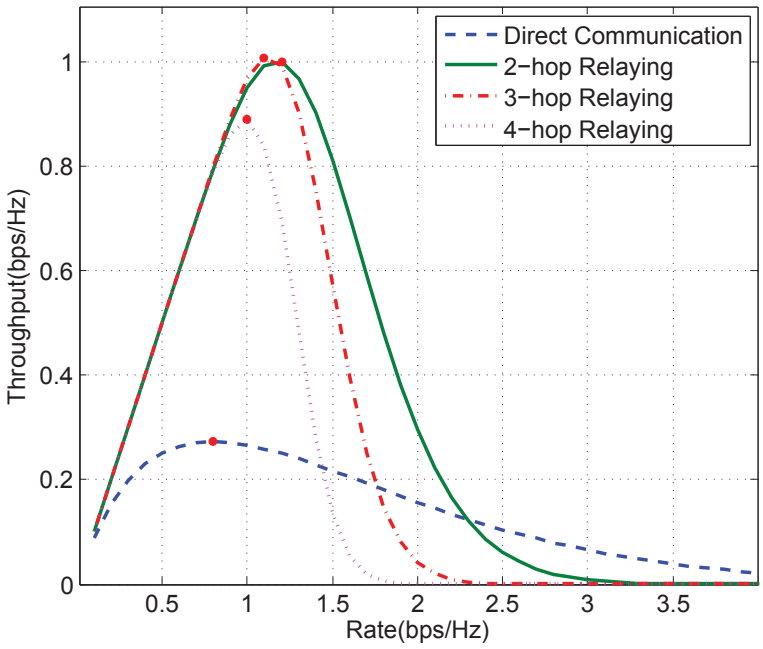

Figure 4.5: Multi-hop relaying throughput and the optimal rate ($\gamma = 12$dB)

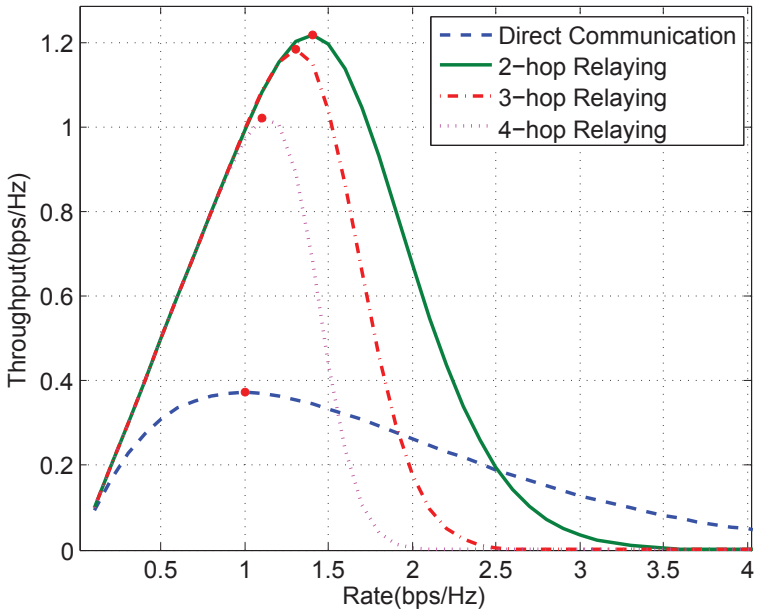

Figure 4.6: Multi-hop relaying throughput and the optimal rate ($\gamma = 16$dB)

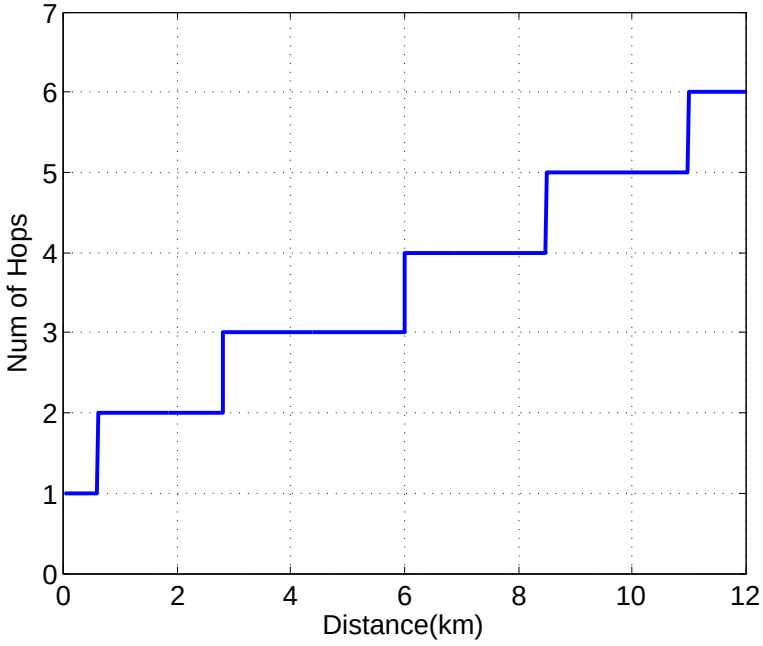

Figure 4.7: The optimal number of hops in terms of the distance

to be 60 and analyze the throughput using the optimal rate in each multi-hop. In both cases, we observe that the optimal number of hops increases linearly as the distance increases. This can be explained from the fact that the path diversity increases as the number of hops increases.

4.5 Conclusions and Future Research

In this chapter we analyzed the exact outage probability of a multi-hop relay network. Based on the outage probability, we also found the optimal rate and the optimal number of hops. Rate control is one of the main forms of transmission adaptation suitable for multi-hop relay communication. We saw that the possible gain of this data adaptation is the higher network throughput. Especially, note that when the SNR is high, thus, the outage probability is relatively low, adapting optimal rate is necessary to improve the overall system throughput.

We also studied the optimal number of hops depending on the distance between the source and the destination. However, there are several challenges that need to be addressed when designing multi-hop relay networks and finding appropriate strategies. For instance, as the number of hops increases, the required time slots or channels should also increase depending on the modulation schemes and the corresponding MAC layer overhead increases as well. It will be worth to investigate the optimal number of hops incorporating the required resources and the overhead of upper layers. Moreover, a low complexity path-selection algorithm should be designed to select an appropriate path.

CHAPTER V

Extension of Relay Communications: Buffer-equipped Relaying and Full Spatial Reuse Multi-hop Relaying

5.1 Introduction

In a conventional opportunistic relay network, the relay selection scheme chooses a relay that has the maximum of the minimum channel gains along the path. This scheme, however, may not use the best channel gain link of each hop. For instance, in a two-hop relay network, a relay is chosen to maximize the minimum of the channel gain between the source-to-relay and relay-to-destination. Thus, the selected relay may not have the maximum source-to-relay channel gain or the maximum relay-to-destination channel gain. To overcome this possible sub-optimality, a buffer-equipped relay network has been recently investigated [23] [48], where the network allows relays to delay transmission and transmit when the channel conditions are favorable. In this network, for an opportunistic relay selection protocol, we consider max-max relay selection (MMRS) protocol [23], where a relay with the maximum channel gain between the source and the relays receives and then stores the source data in its buffer. Then a relay with the maximum channel gain between the relays and the destination forwards the data from its buffer. Thus, two relays are involved in the relaying: one

for a source data reception and the other for a transmission to the destination. Using the best channel in each link improves the outage probability and the throughput especially when the number of relays in the network is large. However, for MMRS to work, the reception relay's buffer must not be filled and the transmission relay's buffer must not be empty. However, a relay selection protocol incorporating this practical buffer issue has been lacking [49][48]. In the following sections, as a relay selection method that resolves the buffer issues, we suggest dual-timer relay selection (DTRS). By adopting the inverse timer algorithm in reception and transmission relay selections, the DTRS algorithm reduces relay selection overhead and solves the full-buffer problem of a reception relay and the empty-buffer problem of a transmission relay in the MMRS protocol.

In recent years, spatial reuse techniques have attracted the attention of the research community thanks to their efficient utilization of the bandwidth of a multi-hop relay network. The research on spatial reuse multi-hop networks to avoid interference from concurrent transmissions has been investigated in [39][28]. This type of spatial reuse requires power adjustment from transmitters and MAC layer control mechanisms. Thus, the maximum allowed spatial reuse factor is 3, which means concurrent transmissions are allowed to relays separated by at least 3 hops. Investigation on the more efficient spatial reuse protocol is needed. As the more efficient spatial reuse technique, we suggest FSRM scheme which allows simultaneous transmissions to relays separated by 2 hops. In a directional antenna system, since relays direct their signal to the intended receiver, the FSRM scheme becomes free from co-channel interference. We examine the exact end-to-end outage probability of the FSRM scheme and compare this with a traditional orthogonal multi-hop relay communication scheme. Further, we analyze the FSRM scheme for node with omnidirectional antennas. The interference is the transmission of the data packet with fading effects of the channel. We focus on the fact that the data is known to a node because it is forwarded in

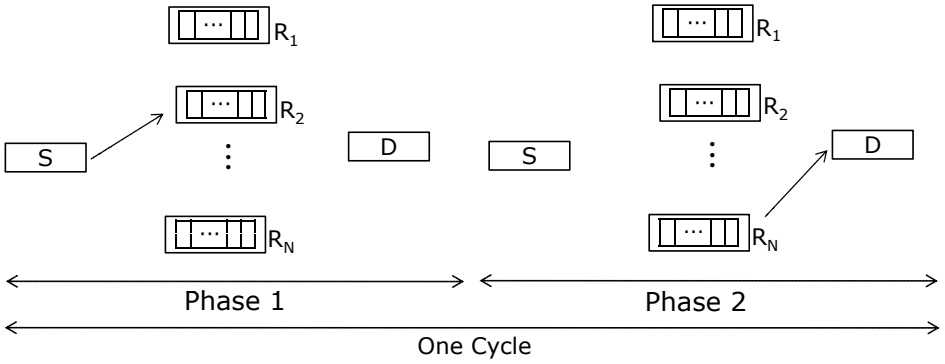

Figure 5.1: Example of a buffer-equipped, multiple-antenna relay communication

the previous time slot by the previous hop node. Thus, the receiver can reduce the interference by estimating the fading level. We find the region of SNR and estimation error where FSRM performs better than the orthogonal relay communication. In the FSRM relay system, not all nodes suffer from interference. For instance, in a 4-hop relay network, the last 2 hops are not interfered with by the other nodes (see Fig. 5.4). This level of difference in interference makes the high interference hop a bottleneck of a multi-hop relay system. To resolve this possible degradation, we investigate power allocation methods in terms of the information allowed in each node.

5.2 Buffer-Equipped Relay Network

5.2.1 System Model

Fig. 5.1 illustrates a two-hop buffer-equipped relay communication network. The system is composed of a source node S, a destination node D, and N number of relays between them, where each node is equipped with a buffer. The channel model that we are assuming is the same as in Section 2.2 in Chapter II. Given the channel model, the received signal can be expressed as follows

$$y[k] = \frac{h[k]\sqrt{L}}{(d/2)^{\frac{\eta}{2}}}\sqrt{\mathrm{E}}x[k] + w[k], \qquad k = 1, ..., K$$

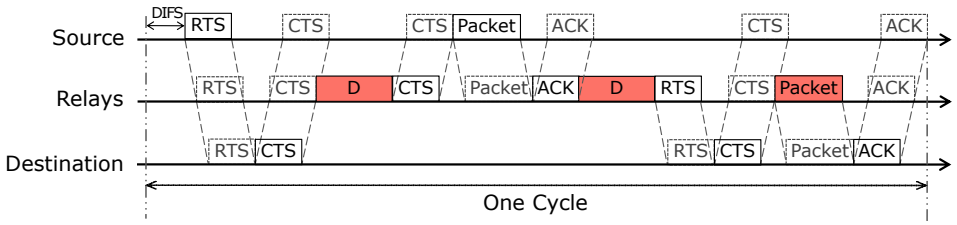

Figure 5.2: MAC layer relay transmission sequences of a buffer-equipped relay network

where $x[k]$ and $y[k]$ are k-th transmitted and received symbols, respectively. The rest of the symbols are defined earlier in Section 2.2.

As shown in Fig. 5.1, in phase 1, the source transmits a data packet, and then the reception relay decodes the data packet and stores the data in its buffer. In phase 2, the transmission relay forwards the data from its buffer. The difference from the conventional opportunistic relay communication is the best channel gain link at each hop can be used in the transmission. This requires executing a relay selection algorithm twice: select a relay to receive the source data and a relay to forward the data. The advantages that arise from this network are examined in Section 5.2.3.

Fig. 5.2 shows the MAC layer transmission sequences of the opportunistic communication of a buffer-equipped relay network. We are assuming that the reception relay selection (RRS) is executed before the data packet transmission to avoid redundant process of flushing the buffers of relays which decode the source data, but are not selected in forwarding the data to the destination. We denote the average time for RRS and transmission relay selection (TRS) as D. The rest of the procedure is the same as the conventional opportunistic relay communication without buffers (see Fig. 2.3).

5.2.2 Relay Selection Criteria and Selection Algorithm

The opportunistic relay communication protocol studied in the previous chapters uses the same relay for the first hop and the second hop [10], which is referred to as BRS.

In this case, the BRS chooses a single relay (I) which has the maximum channel gain from the minimum channel gain of the source-to-relay and relay-to-destination links. For the channel model that we are considering, the capacity depends on the shadow fading level. Thus, a relay that BRS chooses can be defined as follows

$$I = \arg \max_{i=1,\ldots,N} \min(L_{Si}, L_{iD}), \tag{5.1}$$

where L_{Si} and L_{iD} are the shadow fading channel gains between the source to relay i and the relay i to the destination, respectively. Although this relay selection achieves full diversity order [10], this may not use the best of source-to-relay or relay-to-destination links channel gains, because one selected relay receives and forwards the data. To exploit the best channel gains of each links, the MMRS protocol has been suggested in a buffer-equipped relay networks [23]. In the MMRS protocol, the optimal relays for the reception (I_{rx}) and transmission (I_{tx}) are defined as follows

$$I_{rx} = \arg \max_{i=1,\ldots,N} L_{Si}, \quad I_{tx} = \arg \max_{i=1,\ldots,N} L_{iD}.$$

As a practical application of MMRS, hybrid relay selection (HRS) is suggested in [23], which adopts BRS when the buffer of the reception relay is full or the transmitter relay's buffer is empty; otherwise, MMRS is adopted. It is assumed that the relays leave at least one space of its buffer empty so that each is always able to receive in case it is selected for reception when the BRS protocol is used. However, if the buffer of a reception relay (I_{rx}) is full, but the buffer of a transmission relay (I_{tx}) has packet, it is better to use a second best relay for a reception, and use I_{tx} for transmission. For this reason, we suggest DTRS algorithm, which selects next best relays when the buffer of I_{rx} is full or the buffer of I_{tx} is empty. In the DTRS algorithm, relays set their timers only according to their source-to-relay channel gains in the RRS phase. Likewise, in the TRS phase, relays set their timers according to their relay to

destination channel gains. However, the relays with a full buffer in the RRS phase, and the relays with an empty buffer in the TRS phase do not set their timers. Therefore, the DTRS algorithm avoids the buffer issues of MMRS and the selection is executed in a distributed fashion without exchanging CSI.

The DTRS protocol can be adopted in the multi-hop relay network as well. Consider a M-hop relay network, where the number of relays at each hop is N_M as defined in (4.1), and relay clusters are equally spaced as depicted in Fig. 4.1. The first hop reception relay and the M-th hop transmission relay can be found from (5.1). For the m-th hop transmission, where $m \neq 1$ or M, the maximum channel gain link among $(N_M)^2$ links can be defined as follows

$$(I_t^m, I_r^{m+1}) = \arg \max_{i,j=1,\ldots,N_M} L_{R_i^m, R_j^{m+1}}, \tag{5.2}$$

where I_t^m is the transmission relay for the m-th hop, and I_r^{m+1} is the reception relay for the $(m+1)$-th hop. As we defined earlier, R_i^m is the i-th relay at the m-th hop. The performance improvement from having buffers in a multi-hop relay network is analyzed in the following section.

5.2.3 Relay Communication Performance Analysis

The outage probability of a buffer-equipped relay network depends on the size of the buffer of a relay used in the transmission. Analysis on the finite buffer is out of scope of this thesis, but the numerical analysis on the finite buffer is addressed in Section 5.4. For the following analysis, we assume that the buffer size is infinite, thus, the full buffer problem does not occur. We also assume that the relay transmission is initialized by transmitting sufficiently large number of packets to relays before a relay transmits a packet, thus, the empty buffer problem is avoided.

Suppose the source and the selected relay are transmitting at the same rate R

(in bits/s/Hz), where we assume the equal transmission time duration for the first hop transmission and the second hop transmission. Under this assumption, an end-to-end outage is said to occur if the minimum of the capacity of the source to relay and the relay to destination links is less than R. We assume that each of the relays experiences independent shadowing and $L_{SI_{rx}}$ and $L_{I_{tx}D}$ are also independent. We further assume that all the relays are clustered in the midpoint between the source and destination and their distance from each other is negligible when compared to the distance from the source and the destination. Then the outage probability of using the optimal relay is given by

$$\begin{aligned} P_{out}(R) &= Pr\left(\{\min(C(L_{SI_{rx}}), C(L_{I_{tx}D}))\} < R\right) \\ &= 1 - Pr\left(C(L_{SI_{rx}}) > R\right) Pr\left(C(L_{I_{tx}D}) > R\right) \\ &= 1 - \left\{1 - \prod_{i=1}^{N}\left(1 - Q\left(\frac{\ln(g(R))}{\sigma_{Si}}\right)\right)\right\}\left\{1 - \prod_{i=1}^{N}\left(1 - Q\left(\frac{\ln(g(R))}{\sigma_{iD}}\right)\right)\right\}, \end{aligned}$$

where σ_{Si} and σ_{iD} are the standard deviations of the associated normal r.v.s. According to this equation, the outage probability depends on the shadow fading characteristics and the minimum number of antennas between the source (relay) and relay (destination). In addition, the outage probability decreases as the number of relays N increases and the target rate R decreases. For mathematical simplicity, we assume the distribution of the shadow fading of the source to relay and relay to destination are identical. Then, the outage probability can be written as follows

$$P_{out}(R) = 1 - \left(1 - (1 - \mathcal{Q})^N\right)^2,$$

where $\mathcal{Q}$ is defined in (2.29).

In a multi-hop relaying outage analysis, the end-to-end outage probability is said to occur if the minimum of the maximum links of each hop is less than R. Then

the outage probability of a buffer-equipped multi-hop relay network can be found as follows

$$\begin{aligned}
P_{out}(R) &= Pr\left(\min\left\{C(L_{S,R_{I_r}}), C(L_{R_{I_t^2},R_{I_r^3}}), ..., C(L_{R_{I_t},D})\right\} < R\right) \\
&= 1 - Pr\left(\min\left\{C(L_{S,R_{I_r}}), C(L_{R_{I_t^2},R_{I_r^3}}), ..., C(L_{R_{I_t},D})\right\} > R\right) \\
&= 1 - Pr\left(C(L_{S,R_{I_r}}) > R\right) Pr\left(C(L_{R_{I_t^2},R_{I_r^3}}) > R\right), ..., Pr\left(C(L_{R_{I_t},D}) > R\right) \\
&= 1 - \left(1 - (1-\mathcal{Q}_M)^{N_M}\right)\left(1 - (1-\mathcal{Q}_M)^{N_M{}^2}\right), ..., \left(1 - (1-\mathcal{Q}_M)^{N_M}\right) \\
&= 1 - \left(1 - (1-\mathcal{Q}_M)^{N_M}\right)^2 \left(1 - (1-\mathcal{Q}_M)^{N_M{}^2}\right)^{M-2}.
\end{aligned}$$

This end-to-end outage probability analysis is rather simpler than a multi-hop relay network without buffers, because the best channel gain link in each hop is chosen independently from the other hops.

5.2.4 Relay Selection Period

Although the DTRS algorithm described in Section 5.2.2 minimizes the overhead in relay selection, selecting the two optimal relays requires resources corresponding to the initial timer values. Suppose A denotes the number of transmitted bits in one cycle. Let X_m be a r.v. measuring the number of successfully received bits at the destination at cycle m. The throughput of the system with the selection period T, denoted by $S_T(v)$, is given by

$$S_T(v) = \frac{\sum_{m=1}^{T} E[X_m]}{2D + \tau T}.$$

Compared to (3.5), a buffer-equipped relay network requires two selection period, and the expected number of bits $E[X_m]$ successfully received at the destination differed

as follows

$$\begin{aligned} E[X_m] =& E[A1_{\{\text{no outage occurred at cycle } n\}}] \\ &= A(1 - P_{out}(R)) \\ &= A\left(Pr\left(C(L_{m,SI_{rx}(1)}) > R\right) Pr\left(C(L_{m,I_{tx}(1)D}) > R\right)\right), \end{aligned} \tag{5.3}$$

where $L_{m,SI_{rx}(1)}$ and $L_{m,I_{tx}(1)D}$ are the mth cycle lognormal shadowing levels of the source to the optimal reception relay chosen at cycle 1 and the optimal transmission relay at cycle 1 to the destination, respectively. Each of the probabilities in (5.3) is analyzed in appendix A, where the only difference is the inverse function of the capacity.

5.3 Full Spatial Reuse Multi-hop (FSRM) Relay Communication

5.3.1 System Model

In a conventional orthogonal multi-hop relay network, each node transmits its data packet in orthogonal time domain sub-channels. Because of this orthogonal transmission characteristic, in an M-hop relay network, the end-to-end capacity and the per-hop capacity difference is a factor of M. In a spatial reuse multi-hop relay network, nodes are allowed to transmit simultaneously to increase the channel utilization. The channel utilization is represented by the spatial reuse factor [45]. The spatial reuse factor of K means that the relays separated by K-hops are allowed to transmit their data simultaneously. Thus, as the spatial reuse factor increases, the channel utilization decreases. The minimum and the maximum spatial reuse factors are 2 and M, respectively.

We consider a multi-hop relay network, where the spatial reuse factor is 2. We

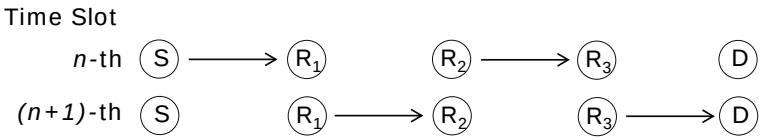

Figure 5.3: Example of FSRM in a directional antenna system

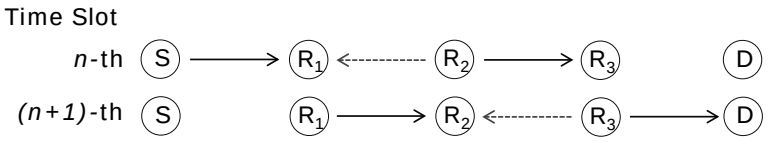

Figure 5.4: Example of FSRM in an omnidirectional antenna system

call this network which allows the maximum channel utilization as a FSRM relay network. In the FSRM relay network, all the odd index hop relays transmit in the same time slot, and then the even index hop relays transmit in the next time slot. For example, Fig. 5.3 and 5.4 illustrate a 4-hop FSRM relay communication. While the source transmits a data packet to relay R_1, relay R_2 transmits its data simultaneously in the n-th time slot. In the $(n+1)$-th time slot, relay R_1 and R_3 forward their data simultaneously. We assume that only the closest neighbor node can hear the transmission. In a directional antenna system, relay R_1 does not overhear data from R_2, and neither does relay R_2 from R_3. However, in an omnidirectional antenna system, R_1 receives data from source and R_2. Thus, the data transmission from R_2 causes interference, where the interference is due to the signal transmitted by R_1 corresponding to the forwarded data in the previous time slot by R_1. Since R_1 knows the data, if the fading level between R_1 and R_2 is perfectly known to R_1, the interference can be cancelled. In this chapter, we assume that R_1 has only the partial information about the fading level, which means the channel estimation between R_1 and R_2 is imperfect.

5.3.2 Directional Antenna System Outage Probability Analysis

In this section, a closed form expression for the directional antenna FSRM relay communication outage probability is derived. A single hop channel model assumed in this section is the same as in Section. 4.2.2. However, we assume the shadow fading L remains constant over a codeword, and i.i.d. across one codeword to another codeword to a better understanding of a spatial reuse multi-hop network. We assume that the CSI is available at the receiver, and that the transmitter has only statistical information. For a given shadowing level L, a single hop capacity of an M-hop relay communication, incorporating the channel effects described above, is found to be [34]

$$\begin{aligned} C\left(\frac{L\gamma_M}{N_0}\right) &= E_{|h|^2}\left\{\log\left(1+|h|^2\,\frac{L\gamma_M}{N_0}\right)\right\} \\ &= \int_0^\infty \log\left(1+x\frac{L\gamma_M}{N_0}\right)e^{-x}dx \\ &= -\frac{e^{\frac{N_0}{L\gamma_M}}}{\ln 2}Ei\left(-\frac{N_0}{L\gamma_M}\right), \end{aligned} \tag{5.4}$$

where $Ei(x)$ is exponential integral defined in (2.5). In a conventional orthogonal multi-hop relay network, each relay transmits every M time slot. Thus, the capacity is reduced by a factor of M. To achieve the end-to-end rate R (in bps/Hz), each hop transmission rate should be MR. An outage occurs, when the target rate per hop MR is greater than the capacity (5.4). The corresponding outage probability is given by

$$\begin{aligned} P_{out}(R) &= Pr\left(C\left(\frac{L\gamma_M}{N_0}\right) < MR\right) \\ &= Pr\left(\Gamma < \ln\frac{N_0 g(MR)}{\gamma_M}\right) \\ &= 1-Q\left(\frac{\ln\frac{N_0 g(MR)}{\gamma_M}}{\sigma}\right), \end{aligned}$$

where Γ is a log scale of lognormal shadowing gain L, and $g(\cdot)$ is the inverse function of the capacity. On the other hand, in the FSRM relay system, when M is even, each relay transmits every other time slot, and the total average energy constraint E is split between $M/2$ relays in each time slot. The capacity for the given shadowing level L, thus, becomes as follows

$$C\left(\frac{2L\gamma_M}{MN_0}\right) = E_{|h|^2}\left\{\log\left(1+\frac{2\left|h\right|^2 L\gamma_M}{MN_0}\right)\right\}. \tag{5.5}$$

However, since each relay transmits every other time slot, the capacity is only reduced by a factor of 2 to obtain the end-to-end rate. Thus, to achieve an end-to-end rate of R, the transmission rate for each hop should be $2R$. If we assume the fast fading and shadowing levels in each hop are the same and constant, we can compare the capacity of the FSRM and orthogonal relay networks as follows

$$\begin{aligned}
\frac{1}{2}\log\left(1+\frac{2\gamma_M}{MN_0}\right) &\underset{FSRM}{\lessgtr} \frac{1}{M}\log\left(1+\frac{\gamma_M}{N_0}\right)\\
\left(1+\frac{2\gamma_M}{MN_0}\right)^{\frac{M}{2}} &\underset{FSRM}{\lessgtr} 1+\frac{\gamma_M}{N_0}\\
\sum_{k=0}^{M/2}\binom{M/2}{k}\left(\frac{2\gamma_M}{MN_0}\right)^k &\underset{FSRM}{\lessgtr} 1+\frac{\gamma_M}{N_0}\\
1+\frac{\gamma_M}{N_0}+\frac{M-2}{2M}\left(\frac{\gamma_M}{N_0}\right)^2\cdots+\left(\frac{2\gamma_M}{MN_0}\right)^{\frac{M}{2}} &\underset{FSRM}{\lessgtr} 1+\frac{\gamma_M}{N_0}\\
\frac{M-2}{2M}(\frac{\gamma_M}{N_0})^2\cdots+\left(\frac{2\gamma_M}{MN_0}\right)^{\frac{M}{2}} &\underset{FSRM}{>} 0.
\end{aligned}$$

When M is greater than 2, this shows that the capacity of the FSRM is always greater than the conventional orthogonal multi-hop. For odd M, $(M+1)/2$ number of odd index hop relays transmit at the same time slot, and in the next time slot, $(M-1)/2$ number of even index hop relays transmit simultaneously. Thus, the capacity for the

odd and even indexed hop relays can be defined respectively as follows

$$\frac{M+1}{2}\log\left(1+\frac{2\gamma_M}{N_0(M+1)}\right),$$
$$\frac{M-1}{2}\log\left(1+\frac{2\gamma_M}{N_0(M-1)}\right).$$

The capacity comparison with the orthogonal transmission scheme can be performed in the same way as the even M-hop transmission.

In this chapter, we analyze the outage probability in a 4-hop relay network. We denote node 1 to be the source, node 2 to be the first hop relay and so on to simplify notation. For a random shadowing channel, an end-to-end outage is said to occur if the minimum capacity among 4 hops is less than each hop target rate. If the end-to-end rate is R, then the orthogonal relay network outage probability is

$$\begin{aligned} P_{out}(R) &= Pr\left(\min\left\{C\left(\frac{L_{n,12}\gamma_M}{N_0}\right),\cdots,C\left(\frac{L_{n+3,45}\gamma_M}{N_0}\right)\right\}<4R\right) \\ &= 1-Q\left(\frac{\ln\frac{N_0 g(4R)}{\gamma_M}}{\sigma}\right)^4, \end{aligned} \tag{5.6}$$

where $L_{n,ij}$ denotes the shadow fading gain between node i and j at n-th time slot, and we assume they are i.i.d. across different time slots and different hops. In the FSRM relay network, on the other hand, if the end-to-end rate R, the outage probability can be found as follows

$$\begin{aligned} P_{out}(R) &= Pr\left(\min\left\{C\left(\frac{L_{n,12}\gamma_M}{2N_0}\right),\cdots,C\left(\frac{L_{n+1,45}\gamma_M}{2N_0}\right)\right\}<2R\right) \\ &= 1-Q\left(\frac{\ln\frac{2N_0 g(2R)}{\gamma_M}}{\sigma}\right)^4. \end{aligned} \tag{5.7}$$

As we proved above, to achieve the same target rate, the FSRM scheme uses less power than the orthogonal scheme, which means the Q-function argument of (5.7)

is less than that of (5.6). Thus the FSRM scheme achieves lower outage probability than the orthogonal transmission scheme.

5.3.3 Omnidirectional Antenna System Outage Probability Analysis

In an FSRM relay network equipped with omnidirectional antennas, co-channel interference occurs. As shown in Fig. 5.4, in the n-th and $(n+1)$-th time slots, the SINR of R_1 and R_2 are reduced, respectively. However, the SINR of R_3 and D are the same as the directional antenna system. Since the end-to-end outage probability is governed by the minimum among M hops, a power allocation scheme can decrease the end-to-end outage by reducing the difference in SINR at each node in the same time slot. In this section, we find the end-to-end outage probability of an FSRM relay network with omnidirectional antennas and analyze power allocation methods with respect to information allowed at each node. For analysis purposes, and to simplify notation, we analyze the system performance of a 4-hop relay network, and denote node 1 to be the source, node 2 to be the first hop relay and so on as before. If the second hop reception relay, node 3, successfully decodes the previous data packet, x_{n-1}, the received signal at the first hop relay, node 2, in n-th time slot, can be written as follows

$$y_n[k] = h_{12}[k]\sqrt{\frac{L_{n,12}\gamma_M}{2}}x_n[k] + h_{32}[k]\sqrt{\frac{L_{n,32}\gamma_M}{2}}x_{n-1}[k] + w[k],$$

where $y_n[k]$ is the received signal in n-th time slot, and the second term of the right-hand-side equation causes interference. Since the data packet x_{n-1} is forwarded by node 2 in $(n-1)$-th time slot, node 2 has information about the interference. Since shadowing is a large scale fading phenomenon, which is caused by the random nature of the interferer location [12], and constant over a time slot, it is reasonable to assume that the shadowing level $L_{n,32}$ is known to node 2. On the other hand, the fast fading

is varying over a time slot, we assume that node 2 can only estimate $h_{32}[k]$ with errors. In MMSE based estimation, the channel can be modeled as a known part with probabilistic additive component as $\hat{h}_{32}[k] = h_{32}[k] + e$, where e denotes the channel estimation error, which has Gaussian distribution with zero mean and σ_e^2 variance. Since the worst effect of the error is to behave as AWGN [30], this channel estimation model is reasonable in the capacity analysis. Incorporating the fading information, node 2, can subtract the interference as follows

$$\begin{aligned} & y_n[k] \\ & = h_{12}[k]\sqrt{\frac{L_{n,12}\gamma_M}{2}}x_n[k] + \left(h_{32}[k]\sqrt{\frac{L_{n,32}\gamma_M}{2}} - \hat{h}_{32}[k]\sqrt{\frac{L_{n,32}\gamma_M}{2}}\right)x_{n-1}[k] + w[k] \\ & = h_{12}[k]\sqrt{\frac{L_{n,12}\gamma_M}{2}}x_n[k] + e\sqrt{\frac{L_{n,32}\gamma_M}{2}}x_{n-1}[k] + w[k]. \end{aligned}$$

We can write a the achievable rate of the first link defined as follows

$$\begin{aligned} C\left(\frac{L_{n,12}\gamma_M}{2N_0}, \frac{L_{n,32}\gamma_M}{2N_0}\right) &= E_{h_{12}}\left\{\log\left(1 + \frac{|h|^2 L_{n,12}\gamma_M}{\sigma_e^2 L_{32}^n \gamma_3 + 2N_0}\right)\right\} \\ &= \int_0^\infty \log\left(1 + \frac{x L_{n,12}\gamma_M}{\sigma_e^2 L_{n,32}\gamma_M + 2N_0}\right) e^{-x} dx \\ &= -\frac{e^{\frac{1}{\gamma_{R_2}}}}{\ln 2} Ei\left(-\frac{1}{\gamma_{R_2}}\right), \end{aligned}$$

where γ_{R_2} is the received SINR at node 2 as follows

$$\gamma_{R_2} = \frac{L_{n,12}\gamma_M}{\sigma_e^2 L_{n,32}\gamma_M + 2N_0}. \tag{5.8}$$

On the other hand, node 4 and node 5 are not interfered by the other transmission. The capacity between node 3 and 4, thus becomes as follows

$$C\left(\frac{L_{n,34}\gamma_M}{2N_0}\right) = E_{h_{34}}\left\{\log\left(1+\frac{|h_{34}|^2 L_{n,34}\gamma_M}{2N_0}\right)\right\}$$
$$= -\frac{e^{\frac{1}{\gamma_{R_4}}}}{\ln 2} Ei\left(-\frac{1}{\gamma_{R_4}}\right),$$

where γ_{R_4} is the received SINR at node 4 as follows

$$\gamma_{R_4} = \frac{L_{n,34}\gamma_M}{2N_0} \tag{5.9}$$

For a comparison with the orthogonal relay scheme, we assume fast fading and shadowing levels for the both cases are fixed as the mean value and the end-to-end rate is fixed as R. Then the comparison can be made as follows

$$\frac{1}{2}\log\left(1+\frac{\gamma_M}{\sigma_e^2\gamma_M+2N_0}\right) \underset{FSRM}{\lessgtr} \frac{1}{4}\log\left(1+\frac{\gamma_T}{N_0}\right)$$
$$\frac{\gamma_M}{N_0} \overset{FSRM}{\lessgtr} \frac{1-2\sigma_e^2}{\sigma_e^4}. \tag{5.10}$$

Since the end-to-end outage probability depends on the minimum channel gain of the multiple hops, comparing the transmission with interference with the orthogonal transmission is enough. When the power of the estimation error is less than $1/2$, there exist a range of SNR ranges such the FSRM relay network achieves higher capacity then the orthogonal relay network. We can also see from (5.10) that as the power of the estimation error decreases, the operating range of SNRs increases. Since we assume that the channel characteristic of each hop is the same, the above analysis holds true for $(n+1)$-th time slot transmission where node 2 and 4 transmit their data simultaneously.

In the previous analysis, we assume the energy constraint is E in each time slot,

and it is equally divided between the relays that transmit simultaneously. Thus, the received energy without interference is $\gamma_M/2$ in 4-hop relay communication. However, in the omnidirection antenna system, because of the interference, the received SINR γ_{R_2} is smaller than γ_{R_4}. Since the end-to-end outage depends on the minimum capacity of each hop, smaller received SINR γ_{R_2} can be a bottle neck of the end-to-end outage probability. Thus, a power allocation method that adjusts the power can decrease the end-to-end outage probability. We define a power allocation parameter α $(0 \leq \alpha \leq 1)$, and the transmission energy for node 1 and 3 as E_1 and E_3, respectively, where

$$\mathrm{E}_1 = (1-\alpha)\mathrm{E}, \qquad \mathrm{E}_3 = \alpha\mathrm{E}.$$

Since we assume the relays are equally spaced, the received SINR at γ_{R_2} and γ_{R_4} can be defined as follows

$$\gamma_{R_2} = \frac{L_{n,12}(1-\alpha)\gamma_M}{\sigma_e^2 L_{n,32}\alpha\gamma_M + N_0}, \qquad \gamma_{R_4} = \frac{L_{n,34}\alpha\gamma_M}{N_0}.$$

If the transmitters have the global CSI, the power allocation can be performed to satisfy $\gamma_{R_2} = \gamma_{R_4}$, and the corresponding α is

$$\alpha = \frac{-(L_{n,34}\gamma_M N_0 + L_{n,12}\gamma_T N_0) + \sqrt{(L_{n,34}\gamma_M N_0 + L_{n,12}\gamma_M N_0)^2 + 4N_0 L_{n,12}L_{n,32}L_{n,34}\gamma_M^3\sigma_e^2}}{2L_{n,32}L_{n,34}(\sigma_e\gamma_M)^2}$$

If the transmitters have the statistical information of the slow fading level, the power allocation can be used to satisfy $E[\gamma_{R_2}] = E[\gamma_{R_4}]$.

$$\begin{aligned} E\left[\frac{(1-\alpha)\gamma_M}{\sigma_e^2\alpha\gamma_M L_{n,32} + N_0}\right] &= \frac{\alpha\gamma_M}{N_0} \\ \Rightarrow \frac{1}{\sigma_e^2\alpha\gamma_M} E\left[\frac{1}{L_{n,32} + \frac{N_0}{\sigma_e^2\alpha\gamma_M}}\right] &= \frac{\alpha}{(1-\alpha)N_0}, \end{aligned} \tag{5.11}$$

where we assume that the shadow fading of each hop is i.i.d. with mean 1. The expectation in (5.11) can be obtained numerically, but the corresponding α is difficult to analyze. To find an analyzable α, we assume the transmitters know the mean and the variance information. Then, the power allocation can be performed to satisfy

$$\frac{(1-\alpha)\gamma_M}{\sigma_e^2\alpha\gamma_M + N_0} = \frac{\alpha\gamma_M}{N_0}.$$

The corresponsing α that satisfy the above equation is

$$\alpha = \frac{-N_0 + \sqrt{N_0^2 + \sigma_e^2\gamma_M N_0}}{\sigma_e^2\gamma_M}. \tag{5.12}$$

As shown in Section 5.4, this power allocation performs almost the same as using the statistical information. According to (5.12), as σ_e^2 or γ_M increases, α decreases, which means as the power of the error increases, more power is allocated to the first hop transmission. Incorporating the power allocation factor, the corresponding outage probability is found as follows

$$\begin{aligned}
&Pr\left(C\left(\frac{L_{n,12}(1-\alpha)\gamma_M}{N_0}, \frac{L_{n,32}\alpha\gamma_M}{N_0}\right) < 2R\right) \\
&\quad = Pr\left(\ln\frac{L_{n,12}(1-\alpha)\gamma_M}{\sigma_e^2 L_{n,32}\alpha\gamma_M + N_0} < \ln g(2R)\right) \\
&\quad = Pr\left(\Gamma_{n,12} - \ln\frac{\sigma_e^2 L_{n,32}\alpha\gamma_M + N_0}{(1-\alpha)\gamma_M} < \ln g(2R)\right) \\
&\quad = \int_{-\infty}^{\infty} Pr\left(\ln\frac{\sigma_e^2 L_{n,32}\alpha\gamma_M + N_0}{(1-\alpha)\gamma_M} > l - \ln g(2R)\right) f_{\Gamma_{n,12}}(l)dl \\
&\quad = \int_{-\infty}^{\infty} Pr\left(L_{n,32} > \frac{e^{l-\ln g(2R)}(1-\alpha)\gamma_M - N_0}{\sigma_e^2\alpha\gamma_M}\right) f_{\Gamma_{n,12}}(l)dl \\
&\quad = \int_{-\infty}^{\infty} Q\left(\frac{\ln\left(e^{l-\ln g(2R)}(1-\alpha)\gamma_M - N_0\right) - \ln\left(\sigma_e^2\alpha\gamma_M\right)}{\sigma}\right) f_{\Gamma_{12}^n}(l)dl \\
&\quad = 1 - \widetilde{Q}(2R, \alpha\gamma_M),
\end{aligned} \tag{5.13}$$

where we define this outage probability as (5.13) to simplify notation. Although we assume the channel is symmetric, where $L_{n,32} = L_{n,23}$, since the shadowing varies independently over different time slots, the outage event at each hop becomes independent. Thus, the corresponding outage probability becomes as follows

$$\begin{aligned} P_{out}(R) &= Pr(\min C(L_{n,12}, L_{n,32}), C(L_{n+1,23}, L_{n+1,43}), C(L_{n,34}), C(L_{n+1,45}) < 2R) \\ &= 1 - Pr(C(L_{n,12}, L_{n,32}) > 2R) Pr(C(L_{n+1,23}, L_{n+1,43}) > 2R) \\ &\qquad\qquad Pr(C(L_{n,34}) > 2R) Pr(C(L_{n+1,45}) > 2R) \\ &= 1 - \widetilde{Q}(2R, \alpha\gamma_M)^2 Q\left(\frac{\ln \frac{N_0 g(2R)}{\alpha\gamma_M}}{\sigma}\right)^2. \end{aligned}$$

5.4 Numerical Results

In this section we present numerical results of a buffer-equipped two-hop relay network and a 4-hop spatial reuse relay network. We assume that the source to destination distance is 1 km, and the path loss exponent η is 3. The mean and the variance of lognormal shadowing are 0 and 10 dB, respectively, and the end-to-end rate R is 1 bits/s/Hz. For the buffer-equipped relay network, we assume that the number of relays is 5.

Fig. 5.5 plots the outage probability of different relay selection schemes with respect to the average received SNR γ, where C_b refers to the size of buffers. The MMRS adapted outage probability serves as the lower bound of other selection protocols, since we assume that the buffer issues do not occur in the MMRS protocol. It is seen that the DTRS outperforms the HRS. This is because of the fact that when the MMRS protocol chooses a relay with full or empty buffer, DTRS selects the relays opportunistically among the relays without full or empty buffer, where the channel gain of the BRS selected relay serves as a lower bound of this opportunistic selection. The performance gap between DTRS and HRS is reduced as the buffer size increases.

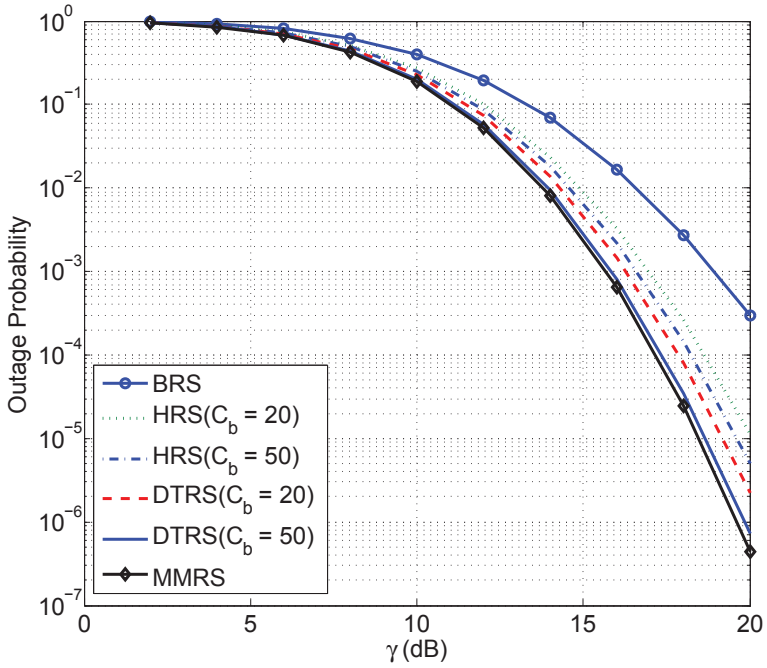

Figure 5.5: Outage probability of BRS, HRS, DTRS, and MMRS

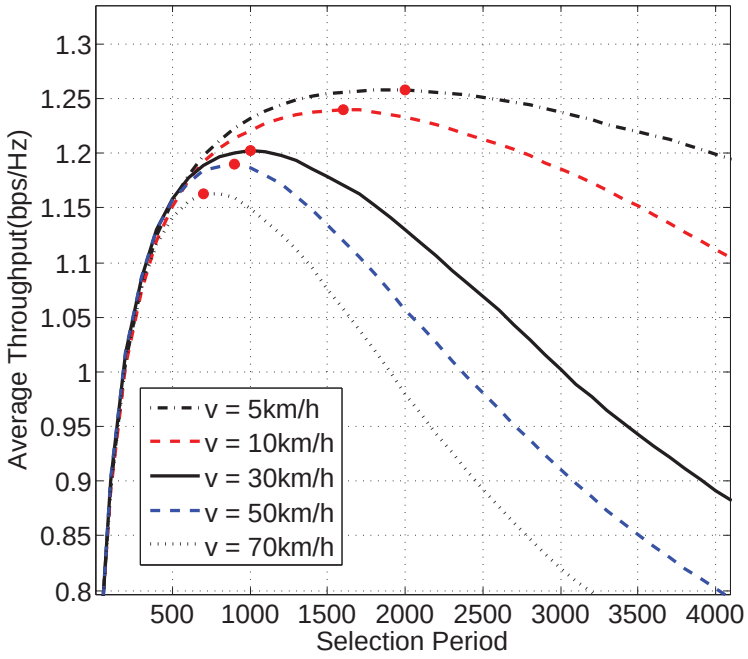

Figure 5.6: The optimal relay selection period of different velocities

This is so because the probability of the relays buffer is full or empty decreases as the buffer size increases.

Fig. 5.6 shows the numerical result of the throughput with different periods and velocities. In this analysis, we assume the average relay selection time for the RRS and TRS is 965 μs. The correlation parameter ϵ_d is 0.15, and the SNR is 18 dB. In Fig. 5.6, the marked points represent the throughput maximizing selection period. We observe that if we select the optimal relay at every cycle (or very often), the throughput does not depend on the vehicle velocity, but it is less than the throughput of the optimal selection period. However, as expected, as the velocity of a vehicle increases, the optimal relay selection period decreases.

From Fig. 5.7, numerical analysis of a 4-hop spatial reuse relay network is provided, where we assume that 3 relays are equally spaced between the source and the destination. Fig. 5.7 shows the boundary of the better performing scheme between the orthogonal transmission and the omnidirectional antenna FSRM transmission scheme in terms of the variance of the estimation error, according to (5.10). The decision of the transmission scheme can be made corresponding to the plot: choose the FSRM transmission scheme on the area under the curve, which is the low SNR region, and choose the orthogonal transmission scheme otherwise. The figure shows that as the variance of the estimation decreases, the SNR region of the FSRM scheme increases. This is because the interference factor $\sigma_e \gamma_M$ in (5.8) remains small for the high SNR because of the low estimation error.

In Fig. 5.8, we compare the power allocation methods using statistical information and mean values in the omnidirectional antenna FSRM system. We used the estimation variance σ_e as 0.1. In the figure, Omni-Ant FSRM PA stands for omnidirectional antenna FSRM power allocation. Although we assume that the transmitter has the statistical information of the fading level, evaluation of the power allocation parameter (α) is complex. We only can find the α numerically. As an alternative,

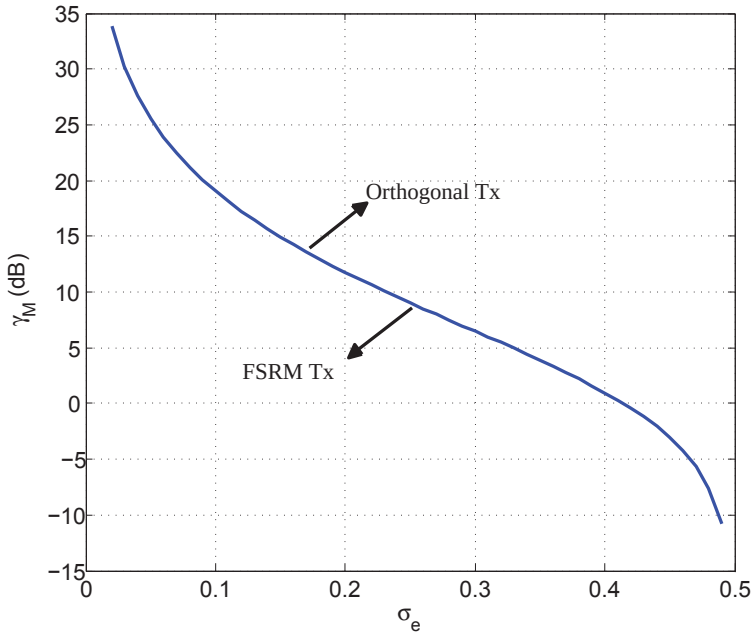

Figure 5.7: The SNR region of transmission schemes in terms of the estimation error

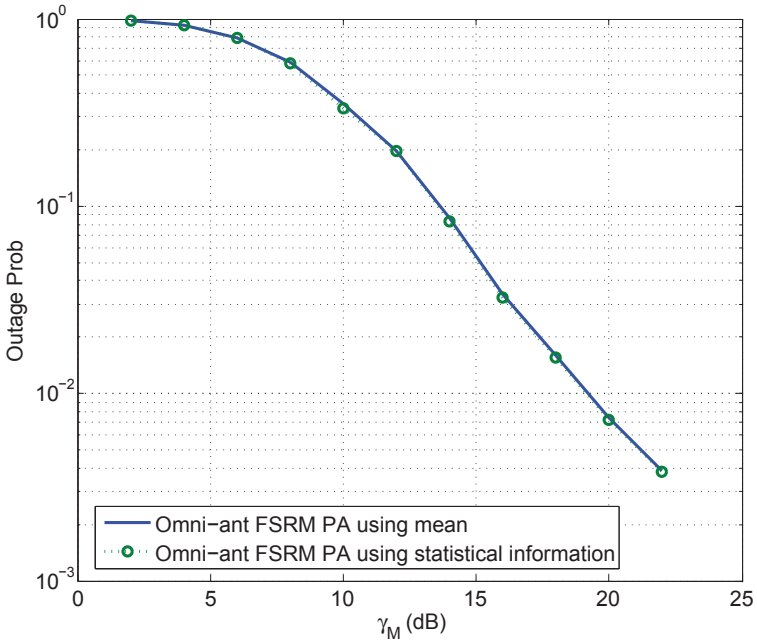

Figure 5.8: Power allocation comparison between using statistical information and using mean values

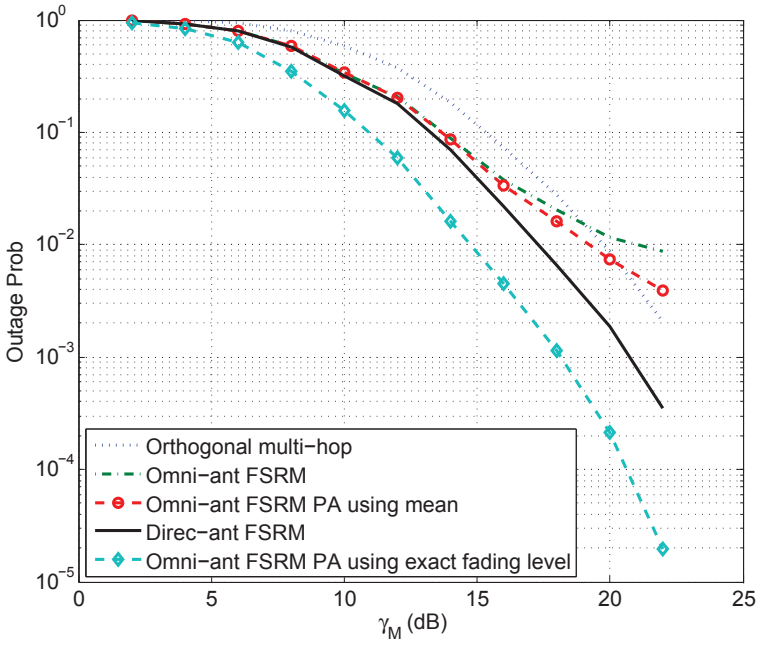

Figure 5.9: Outage probability comparison of the various multi-hop transmission schemes

we find α assuming that the transmitter has only the information of the mean. As shown in the figure, the power allocation scheme using the mean values achieves the same performance as the power allocation using the statistical information. Thus, throughout the following analysis, we compare the power allocation using the mean values with the other multi-hop transmission schemes.

Fig. 5.9 shows the outage probability comparison for the multi-hop relay communication schemes studied in Section 5.3.2, where the variance of the estimation error is 0.1. According to Fig. 5.8, when the variance of the estimation error is 0.1, the FSRM performs better than the orthogonal transmission in the SNR below 18 dB. This is verified in Fig. 5.9 that the crossing point of the orthogonal multi-hop transmission and the omnidirectional FSRM outage probability curves is at 10 dB SNR. This figure also shows that the power allocation using mean values increases the region where FSRM achieves better performance by 2 dB. On the other hand, if the relays are equipped with directional antennas, using 2 dB less SNR, the FSRM

scheme achieves the same outage probability as the orthogonal multi-hop scheme. According to the figure, the outage probability of the omnidirectional antenna FSRM power allocation using the exact fading values achieves better performance than the directional antenna FSRM. Since the power allocation makes the instantaneous channel gains of each hop the same, allocating power can effectively reduce the effect of the estimation error.

5.5 Conclusion and Future Research

In this chapter, we employ a buffering concept at the relay to minimize the end-to-end outage probability. We adopted the distributed timer algorithm as a relay selection method in MMRS, and suggested a new selection algorithm called DTRS, which provides lower outage probability than HRS. We further analyzed the effects of fast and slow fading in the relay selection period in terms of maximizing throughput. The observation that the shadowing is a time-correlated random process allows the relay selection of a buffer-equipped relay to be executed in a certain interval of packet transmissions.

We have also proposed the FSRM scheme, which maximizes spatial reuse in multi-hop relay communication. In our analysis, we considered a directional antenna system and an omnidirectional antenna system. The directional antenna system FSRM always outperforms the conventional orthogonal multi-hop system, and the omnidirectional antenna system performs better than the orthogonal multi-hop system for the low SNR region. The boundary of the region depends on the estimation error. We have shown that the region of the FSRM that performs better increases as the variance of the estimation error decreases. In a 4-hop omnidirectional antenna system, the outage probabilities of the last two links are lower than the orthogonal multi-hop system, but the first two links are the bottle necks of the performance because they suffer from interference. This observation allows us to investigate a power allocation

strategy. Using only the statistical information of the fading, we have shown that the power allocation increases the region where the FSRM performs better.

There are several possible future research directions regarding this multi-hop wireless networks. We assumed the linear multi-hop relay model, where there is one relay in each hop. Developing our analysis with randomly spaced multiple relays will be the direction of the future research. In this model, data routing or relay selection in each hop should incorporate the interference as well as channel gains.

CHAPTER VI

Conclusion

Problems in cooperative communication continue to intrigue researchers by their difficulty and potential for faster and more reliable communication. A myriad of challenging problems need to be solved in the study of cooperative communication. In this thesis, we proposed practical cooperative diversity schemes that employee multiple relay radios. We anticipate that our proposed relay communication schemes and our associated outage probability analyses which incorporate realistic channel effects will enable the design of effective cooperative diversity networks.

In cooperative wireless communication environments, the wireless nodes take advantage of the broadcast nature of the wireless medium. This broadcast nature allows higher spatial diversity and higher throughput. In this area, cross-layer designs introduce efficient relay selection algorithm and help to find the time period of executing the algorithm. It is interesting to find out that executing a relay selection algorithm in the optimal time interval maintains the system throughput close to the optimal even for a user with high mobility. This finding suggests that finding an optimal relay selection period is as important as using an optimal relay selection scheme.

We studied multi-hop relay network with emphasis on the exact end-to-end outage probability. We also found the optimal rate and the optimal number of hops to improve the overall network performance. We saw that adapting rate is necessary

to improve the throughput especially when the SNR is high. One possible extension of this multi-hop scheme is to investigate dynamic path selection for randomly located relays. The linear multi-hop model used is suitable for routing in multi-hop infrastructure-based network. However, for a network with mobile relay station, where relays could be randomly located and their density could be vary from the source and the destination, the linear model is too idealized. Finding a relaying strategy and its outage probability of a mobile relay network will be an interesting challenge.

There is considerable amount of efforts in the research community to improve the end-to-end throughput of relay networks. Buffer-equipped relay networks are receiving special attention at present due to the improvements of throughput they offer compared with conventional relay network. We showed that having buffers at relays gives rise to additional flexibility to cooperative diversity schemes. In addition, the proposed DTRS scheme efficiently resolves buffer issues in the relay selection. Still a lot remains to be accomplished to analyze the performance limits of a network with a finite buffer, and investigating this area will be an interesting topic of future research.

We have also studied multi-hop relay network and proposed a spatial reuse technique, and proposed FSRM which maximize channel resources. There are number of open issues remaining for spatial reuse techniques, such as finding a reuse technique for a network with multiple relays in each hop. However, we anticipate that our current understanding of the principles of cooperative network, together with suggested cooperation protocols will enable more efficient and robust cooperative communication network.

APPENDIX

APPENDIX A

Evaluation of $E[X_m]$

Since we transmit A bits in one cycle, X_m can be expressed as a indicator functions as follows:

$$X_m = A1_{\{\text{no outage occurred at cycle } m\}}.$$

Since the destination has mobility, once the relay is selected, it is reasonable to assume that the source to relay link is always successful. Thus, during a relay selection period, the outage probability of the relay to destination link varies according to the velocity of the destination. Then, the expectation $E[X_m]$ is given by

$$\begin{aligned} E[X_m] &= E[A1_{\{\text{no outage occurred at cycle } m\}}] \\ &= APr\left(L_{m,I(1)} > g(R)\right), \end{aligned} \tag{A.1}$$

where $g(R)$ is inverse function of $f(L)$ defined in (2.4). We take logarithm in both sides of the probability arguments in (A.1). Then, from the law of total probability,

the probability (A.1) becomes:

$$\begin{aligned} & Pr\left(\Gamma_{m,I(1)} > \ln(g(R))\right) \\ &= \sum_{i=1}^{N} Pr\left(\Gamma_{m,i} > \ln(g(R)), I(1) = i\right) \\ &= \sum_{i=1}^{N} Pr\left(\Gamma_{m,i} > \ln(g(R)), \Gamma_{1,i} > \max_{k \neq i} \Gamma_{1,k}\right), \end{aligned} \tag{A.2}$$

where we assume that the number of relays that correctly decodes the source data is N. The probability in (A.2) can be analyzed as follows

$$\begin{aligned} & Pr(\Gamma_{m,i} > \ln(g(R)), \Gamma_{1,i} > \max_{k \neq i} \Gamma_{1,k}) \\ &= \int_{-\infty}^{\infty} Pr(\Gamma_{m,i} > \ln(g(R)), x > \max_{k \neq i} \Gamma_{1,k} | \Gamma_{1,i} = x) f_{\Gamma_{1,i}}(x) dx \\ &= \int_{-\infty}^{\infty} Pr(\Gamma_{m,i} > \ln(g(R)) | \Gamma_{1,i} = x) Pr(x > \max_{k \neq i} \Gamma_{1,k}) f_{\Gamma_{1,i}}(x) dx \\ &= \int_{-\infty}^{\infty} Q\left(\frac{\ln(g(R)) - \rho((m-1)\tau)x}{\sqrt{(1-\rho((m-1)\tau)^2)\sigma^2}}\right) \left(1 - Q\left(\frac{x}{\sigma}\right)\right)^{N-1} f_{\Gamma_{1,i}}(x) dx. \end{aligned} \tag{A.3}$$

where we assume that the shadowing is i.i.d. across the different relays. When $n = 1$, (A.3) becomes

$$Pr(\Gamma_{1,i} > \ln(g(R)), \Gamma_{1,i} > \max_{k \neq i} \Gamma_{1,k}) = \int_{\ln g(R)}^{\infty} \left(1 - Q\left(\frac{x}{\sigma}\right)\right)^{N-1} f_{\Gamma_{1,i}}(x) dx.$$

BIBLIOGRAPHY

BIBLIOGRAPHY

[1] N. Ahmed and Behnaam Aazhang. Throughput Gains Using Rate and Power Control in Cooperative Relay Networks. *IEEE Trans. Commun.*, 55(4):656–660, Apr. 2007.

[2] B. Alawieh, Yongning Zhang, C. Assi, and H. Mouftah. Improving Spatial Reuse in Multihop Wireless Networks - A Survey. *IEEE Commun. Surveys Tutorials*, 11(3):71–91, 2009.

[3] M.S. Alouini and A.J. Goldsmith. Capacity of Rayleigh Fading Channels Under Different Adaptive Transmission and Diversity-Combining Techniques. *IEEE Trans. Vehicular Technology,*, 48(4):1165–1181, July 1999.

[4] R. Babaee and N.C. Beaulieu. Cross-Layer Design for Multihop Wireless Relaying Networks. *IEEE Trans. Wireless Commun.*, 9(11):3522–3531, Nov. 2010.

[5] Changhoon Bae and W.E. Stark. Minimum Energy-per-Bit Wireless Multi-hop Networks with Spatial Reuse. *Journal of Commun. and Networks*, 12(2):103–113, Apr. 2010.

[6] B. Barua, F. Safaei, and M. Abolhasan. On the Outage of Multihop Parallel Relay Networks. In *IEEE Vehicular Technology Conf. (VTC)*, pages 1–5, Sep. 2010.

[7] A.S. Behbahani, R. Merched, and A.M. Eltawil. Optimizations of a MIMO Relay Network. *IEEE Trans. Signal Process.*, 56(10):5062–5073, Oct. 2008.

[8] A. Bletsas, A. Khisti, D.P. Reed, and Andrew Lippman. A Simple Cooperative Diversity Method Based on Network Path Selection. *IEEE JSAC*, 24(3):659–672, 2006.

[9] A. Bletsas, A. Lippnian, and D.P. Reed. A Simple Distributed Method for Relay Selection in Cooperative Diversity Wireless Networks, Based on Reciprocity and Channel Measurements. In *IEEE Vehicular Tech. Conf. (VTC)*, volume 3, pages 1484–1488, 2005.

[10] A. Bletsas, Hyundong Shin, and M.Z. Win. Cooperative Communications with Outage-Optimal Opportunistic Relaying. *IEEE Trans. Wireless Commun.*, 6(9):3450–3460, Sep. 2007.

[11] H. Bolcskei, R.U. Nabar, O. Oyman, and A.J. Paulraj. Capacity Scaling Laws in MIMO Relay Networks. *IEEE Trans. Wireless Commun.*, 5(6):1433–1444, Jun. 2006.

[12] P. Cardieri. Modeling Interference in Wireless Ad Hoc Networks. *IEEE Commun. Surveys Tutorials*, 12(4):551–572, Quarter 2010.

[13] D. Chizhik, G.J. Foschini, M.J. Gans, and R.A. Valenzuela. Keyholes, Correlations, and Capacities of Multielement Transmit and Receive Antennas. *IEEE Trans. Wireless Commun.*, 1(2):361–368, 2002.

[14] Jaeweon Cho and Z.J. Haas. On The Throughput Enhancement of the Downstream Channel in Cellular Radio Networks Through Multihop Relaying. *IEEE JSAC*, 22(7):1206–1219, Sept. 2004.

[15] G. Farhadi and N.C. Beaulieu. Ergodic Capacity of Multi-Hop Wireless Relaying Systems in Rayleigh Fading. In *Proc. IEEE GLOBECOM*, pages 1–6, Dec. 2008.

[16] A. Goldsmith, S.A. Jafar, N. Jindal, and S. Vishwanath. Capacity Limits of MIMO Channels. *IEEE JSAC*, 21(5):684–702, Jun. 2003.

[17] M. Gudmundson. Correlation Model for Shadow Fading in Mobile Radio Systems. *IEEE Lett.*, 27(23):2145–2146, Nov. 1991.

[18] Bo Gui, Lin Dai, and L.J. Cimini. Routing Strategies in Multihop Cooperative Networks. *IEEE Trans. Wireless Commun.*, 8(2):843–855, Feb. 2009.

[19] Xin He and F.Y. Li. Cooperative RTS/CTS MAC with Relay Selection in Distributed Wireless Networks. *Proc. IEEE Int. Conf. Ultra Modern Telecommun. (ICUMT) Workshop*, pages 1–8, Oct. 2009.

[20] L. Hoesel and P. Havinga. Collision-free Time Slot Reuse in Multi-hop Wireless Sensor Networks. In *Int. Conf. on Intelligent Sensors, Sensor Networks and Information Processing Conference*, pages 101–107, Dec. 2005.

[21] Bengt Holter. On The Capacity of The MIMO Channel - A Tutorial Introduction. *Dept. Telecommun., Norwegian Univ. Sci. Tech.*, 2001.

[22] A.S. Ibrahim, A.K. Sadek, Weifeng Su, and K.J.R. Liu. Cooperative Communications with Relay-Selection: When to Cooperate and Whom to Cooperate with? *IEEE Trans. Wireless Commun.*, 7(7):2814–2827, July 2008.

[23] Aissa Ikhlef, Diomidis S. Michalopoulos, and Robert Schober. Max-Max Relay Selection for Relays with Buffers. *IEEE Trans. Wireless Commun.*, 11(3):1124–1135, Mar. 2012.

[24] S.K. Jayaweera and H.V. Poor. Capacity of Multiple-Antenna Systems with Both Receiver and Transmitter Channel State Information. *IEEE Trans. Info. Theory*, 49(10):2697–2709, Oct. 2003.

[25] Y. Jing and H. Jafarkhani. Distributed Differential Space-Time Coding for Wireless Relay Networks. *IEEE Trans. Commun.*, 56(7):1092–1100, July 2008.

[26] David B. Johnson, David A. Maltz, and Josh Broch. The Dynamic Source Routing Protocol for Multi-Hop Wireless Ad Hoc Networks. In *In Ad Hoc Networking, edited by Charles E. Perkins, Chapter 5*, pages 139–172. Addison-Wesley, 2001.

[27] Jean Marc Kelif and Marceau Coupechoux. Joint Impact of Path loss Shadowing and Fast Fading - An Outage Formula for Wireless Networks. *Computing Research Repository (CoRR)*, 2010.

[28] Ting-Yu Lin and J.C. Hou. Interplay of Spatial Reuse and SINR-Determined Data Rates in CSMA/CA-Based, Multi-Hop, Multi-Rate Wireless Networks. In *Proc. IEEE INFOCOM*, pages 803–811, 2007.

[29] R. Madan, N. Mehta, A. Molisch, and Jin Zhang. Energy-Efficient Cooperative Relaying over Fading Channels with Simple Relay Selection. *IEEE Trans. Wireless Commun.*, 7(8):3013–3025, Aug. 2008.

[30] M. Medard. The Effect upon Channel Capacity in Wireless Communications of Perfect and Imperfect Knowledge of the Channel. *IEEE Trans. Info. Theory*, 46(3):933–946, May 2000.

[31] A. Moco, S. Teodoro, A. Silva, and A. Gameiro. Performance Evaluation of Virtual MIMO Schemes for the UL OFDMA Based Systems. In *IEEE Int. Conf. on Wireless and Mobile Commun. (ICWMC)*, pages 71–76, 2008.

[32] O. Oyman and S. Sandhu. A Shannon-Theoretic Perspective on Fading Multihop Networks. *Proc. IEEE Conf. Inf. Sciences and Systems (CISS)*, pages 525–530, Mar. 2006.

[33] L.H. Ozarow, S. Shamai, and A.D. Wyner. Information Theoretic Considerations for Cellular Mobile Radio. *IEEE Trans. Vehicular Technology,*, 43(2):359–378, May 1994.

[34] Sungjoon Park and W.E. Stark. Opportunistic Relaying in Multipath and Slow Fading Channels: Relay Selection and Optimal Relay Selection Period. In *Proc. IEEE MILCOM*, pages 661–666, Nov. 2011.

[35] Xiangping Qin and R. Berry. Opportunistic Splitting Algorithms for Wireless Networks. *Proc. INFOCOM*, 3:1662–1672, Mar. 2004.

[36] E.M. Royer and Chai-Keong Toh. A Review of Current Routing Rrotocols for Ad Hoc Mobile Wireless Networks. *Personal Commun. IEEE*, 6(2):46–55, Apr. 1999.

[37] A. Scaglione, D.L. Goeckel, and J.N. Laneman. Cooperative Communications in Mobile Ad Hoc Networks. *IEEE Signal Processing Magazine*, 23(5):18 – 29, Sept. 2006.

[38] V. Shah, N.B. Mehta, and R. Yim. The Relay Selection and Transmission Tradeoff in Cooperative Communication Systems. *IEEE Trans. Wireless Commun.*, 9(8):2505–2515, Aug. 2010.

[39] Tae suk Kim. Improving Spatial Reuse Through Tuning Transmit Power, Carrier Sense Threshold, and Data Rate in Multihop Wireless Networks. In *Proc. IEEE MobiCom*, pages 366–377. ACM Press, 2006.

[40] R. Tannious and A. Nosratinia. Spectrally-Efficient Relay Selection with Limited Feedback. *IEEE JSAC*, 26(8):1419–1428, Oct. 2008.

[41] Emre Telatar. Capacity of Multi-Antenna Gaussian Channels. *European Trans. on Telecommun.*, 10(6):585–595, 1999.

[42] K. Tourki, M.-S. Alouini, and L. Deneire. Blind Cooperative Diversity Using Distributed Space-Time Coding in Block Fading Channels. *IEEE Trans. Commun.*, 58(8):2447–2456, Aug. 2010.

[43] D. Tse and P. Viswanath. *Fundamentals of Wireless Communications*. Cambridge University Press, 2005.

[44] J.L. Vicario, A. Bel, J.A. Lopez-Salcedo, and G. Seco. Opportunistic Relay Selection with Outdated CSI: Outage Probability and Diversity Analysis. *IEEE Trans. Wireless Commun.*, 8(6):2872–2876, 2009.

[45] Hao Xiao, Yao Fend and L. J. Cimini. Spatial Reuse in Multi-hop Linear Wireless Cooperative Networks. In *Proc. IEEE MILCOM*, Oct. 2012. To appear.

[46] Weiliang Zeng, Chengshan Xiao, Youzheng Wang, and Jianhua Lu. Opportunistic Cooperation for Multi-Antenna Multi-Relay Networks. *IEEE Trans. Wireless Commun.*, 9(10):3189–3199, Oct. 2010.

[47] Wei Zhang and K. Ben Letaief. Opportunistic Relaying for Dual-Hop Wireless MIMO Channels. In *Proc. IEEE GLOBECOM*, pages 1–5, Dec. 2008.

[48] N. Zlatanov and R. Schober. Buffer-Aided Relaying with Adaptive Link Selection-Fixed and Mixed Rate Transmission. *IEEE Trans. Inf. Theory*, 59(5):2816–2840, 2013.

[49] N. Zlatanov, R. Schober, and P. Popovski. Throughput and Diversity Gain of Buffer-Aided Relaying. In *Proc. IEEE GLOBECOM*, pages 1–6, 2011.